

**APPLICATION OF SUGARCANE BAGASSE ASH
MIXTURES FOR SALT AND POTASH
MINE SEALING**



**A Thesis Submitted in Partial Fulfillment of the Requirements for the
Degree of Master of Engineering in Civil, Transportation and
Geo-resources Engineering
Suranaree University of Technology
Academic Year 2016**

การประยุกต์ใช้ส่วนผสมเถ้าขานอ้อยสำหรับบดในช่องเหมืองเกลือและ
เหมืองโพแทช

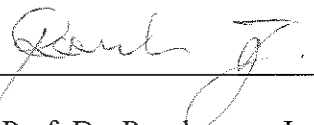


วิทยานิพนธ์นี้เป็นส่วนหนึ่งของการศึกษาตามหลักสูตรปริญญาวิศวกรรมศาสตรมหาบัณฑิต
สาขาวิชาวิศวกรรมโยธา ขนส่ง และทรัพยากรธรณี
มหาวิทยาลัยเทคโนโลยีสุรนารี
ปีการศึกษา 2559

**APPLICATION OF SUGARCANE BAGASSE ASH MIXTURES
FOR SALT AND POTASH MINE SEALING**

Suranaree University of Technology has approved this thesis submitted in partial fulfillment of the requirements for a Master's Degree.

Thesis Examining Committee



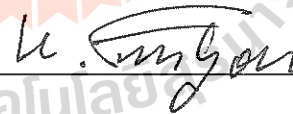
(Assoc. Prof. Dr. Pornkasem Jongpradist)

Chairperson



(Asst. Dr. Decho Phueakphum)

Member (Thesis Advisor)



(Prof. Dr. Kittitep Fuenkajorn)

Member



(Prof. Dr. Sukit Limpijumnong)

Vice Rector for Academic Affairs
and Innovation



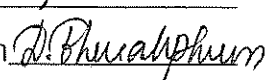
(Assoc. Prof. Flt. Lt. Dr. Kontorn Chamniprasart)

Dean of Institute of Engineering

อี อี ชาน : การประยุกต์ใช้ส่วนผสมเถ้าชานอ้อยสำหรับอุดในช่องเหมืองเกลือและเหมืองโพแทช (APPLICATION OF SUGARCANE BAGASSE ASH MIXTURES FOR SALT AND POTASH MINE SEALING) อาจารย์ที่ปรึกษา : ผู้ช่วยศาสตราจารย์ ดร.เดโช เผือกภูมิ, 65 หน้า.

งานวิจัยนี้ศึกษาการใช้เถ้าชานอ้อยเป็นวัสดุทดแทนซีเมนต์เพื่ออุดในช่องเหมืองเกลือและเหมืองโพแทช โดยส่วนผสมประกอบด้วยเถ้าชานอ้อย ปูนซีเมนต์ปอร์ตแลนด์ เบนโทไนท์และเกลือหินบด การทดสอบกำลังและความแข็งแรงของวัสดุผสมได้ถูกดำเนินการเพื่อนำมาใช้ในการประเมินประสิทธิภาพการลดขนาดการทรุดตัวของผิวดินในเหมืองเกลือและเหมืองโพแทช “วัสดุซีเมนต์” ผสมระหว่างเถ้าชานอ้อยกับปูนซีเมนต์ปอร์ตแลนด์ ในอัตราส่วนเท่ากับ 20:80 โดยน้ำหนัก และเบนโทไนท์ผสมเกลือหินบดในอัตราส่วนเท่ากับ 30:70 โดยน้ำหนัก โดยกำหนดให้ส่วนผสมของ “วัสดุซีเมนต์” ต่อ “เบนโทไนท์ผสมเกลือหินบด” มีอัตราส่วน 1:2 (CPB-1) และ 1:3 (CPB-2) ในการทดสอบใช้สัดส่วนของน้ำเกลือเข้มข้นต่อวัสดุผสมทั้งหมดมีค่าเท่ากับ 0.4 การทดสอบกำลังอัดแกนเดียว (UCS) และกำลังอัดแบบสามแกน (TRI) และการทดสอบกำลังรับแรงดึงแบบบราซิล (BZ) ถูกทดสอบกับตัวอย่างที่ผ่านการบ่มด้วยระยะเวลา 3, 7, 14 และ 28 วัน ผลที่ได้จากการทดสอบถูกนำมาใช้การคำนวณด้วยโปรแกรม FLAC เพื่อจำลองพฤติกรรมในเชิงเวลาของช่องเหมืองในชั้นเกลือและโพแทชที่ถูกอุดด้วยวัสดุผสมนี้ จากผลการทดสอบพบว่าค่ากำลังอัดในแกนเดียวและกำลังดึงแบบบราซิลหลังจากผ่านการบ่มด้วยระยะเวลา 28 วัน สำหรับตัวอย่างที่ผสม “วัสดุซีเมนต์” ต่อ “เบนโทไนท์ผสมเกลือหินบด” อัตราส่วน 1:2 (CPB-1) มีค่าเท่ากับ 7 MPa และ 1.02 MPa และสำหรับอัตราส่วน 1:3 (CPB-2) มีค่าเท่ากับ 5 MPa และ 0.86 MPa ตามลำดับ ผลระบุว่าส่วนผสม CPB-1 มีกำลังสูงกว่าส่วนผสม CPB-2 ค่าความเค้นยึดติดและมุมเสียดทานภายในของตัวอย่างมีค่าเพิ่มขึ้นในช่วงสองสัปดาห์แรกและมีแนวโน้มคงที่หลังจาก 28 วัน ค่าสัมประสิทธิ์ความยืดหยุ่นและอัตราส่วนปัวซองมีการเพิ่มขึ้นเพียงเล็กน้อย การวิเคราะห์ด้วยแบบจำลองทางคอมพิวเตอร์ที่ใช้ผลการทดสอบของตัวอย่างส่วนผสม CPB-2 พบว่าการทรุดตัวของผิวดินลดลงประมาณ 46% เมื่อเทียบกับกรณีที่ไม่มีการอุดช่องเหมือง

สาขาวิชา เทคโนโลยีธรณี
ปีการศึกษา 2559

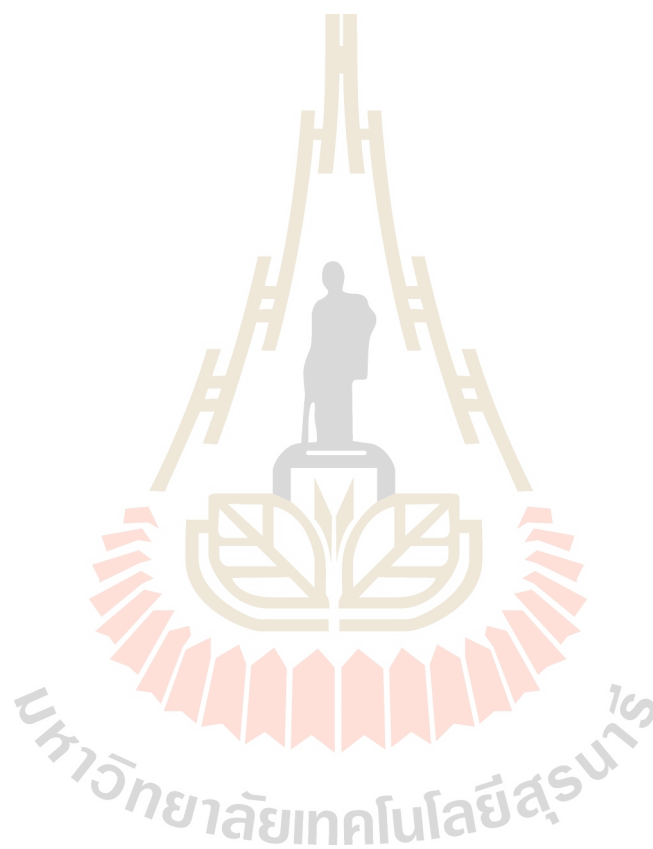
ลายมือชื่อนักศึกษา 
ลายมือชื่ออาจารย์ที่ปรึกษา 

EI EI SAN : APPLICATION OF SUGARCANE BAGASSE ASH
MIXTURES FOR SALT AND POTASH MINE SEALING. THESIS
ADVISOR : ASST. PROF. DECHO PHUEAKPHUM, Ph.D., 65 PP.

SUGARCANE BAGASSE ASH/CEMENTED PASTE BACKFILL/STRENGTH
DEVELOPMENT/SUBSIDENCE

This research investigates the utilization of sugarcane bagasse ash (SCBA) mixed with Portland cement, bentonite and crushed salt as sealing materials to reduce the subsidence in salt and potash mine. The strength and toughness of the mixture are determined here. The ratio of SCBA to cement (cementitious materials) is 20:80 by weight and bentonite to crushed salt (bentonite-crushed salt mixture) is 30:70 by weight. The mixture ratios of cementitious materials to bentonite-crushed salt mixture are 1:2 (CPB-1) and 1:3 (CPB-2). The constant saturated brine-to-mixed materials ratio of 0.4 is used for blending. The uniaxial compressive strength (UCS) test, triaxial compression (TRI) test and Brazilian tensile strength (BZ) test are performed for each curing period of 3, 7, 14 and 28 days. The test results are used in FLAC program to simulate the time dependent behaviors of salt and potash mine with sealing materials. In this study, the UCS and BZ of CPB-1 mixture provides 7 MPa and 1.02 MPa while CPB-2 mixture gives 5 MPa and 0.86 MPa at a curing period of 28 days. The results clearly show that CPB-1 mixture can produce more strength than CPB-2 mixture. The cohesion (c) and internal friction angle (ϕ) are gradually increased at the first two weeks and then tend to remain constant after 28 days. The elastic moduli and Poisson's ratio are slightly increased. From the numerical analysis,

the result obtained from the mine opening with the CPB-2 sealing can reduce the magnitude of subsidence about 46% as compared with that without backfills.



School of Geotechnology

Academic Year 2016

Student's Signature *[Signature]*

Advisor's Signature *D. Thueakplun*

ACKNOWLEDGMENTS

I would like to express my sincerest appreciation and great respect to Asst. Prof. Dr. Decho Phueakphum, my thesis advisor, for supporting with his valuable guidance, amiable encouragement, efficient supervision, forthright suggestions and constructive comments throughout the entire of my research period.

I also would like to acknowledge my grateful thanks to my thesis committee members; Prof. Dr. Kittitep Fuenkajorn and Assoc. Prof. Dr. Pornkasem Jongpradist, and Dr. Prachya Tepnarong for their worthwhile insight, affable encouragement and advice in bringing about my research works.

My acknowledgement is also expressed for the funding supported by Suranaree University of Technology (SUT) and Thailand International Cooperation Agency (TICA).

Further appreciation is acclaimed to all the staffs of Geomechanics Research Unit, Institute of Engineering who supported me to achieve my experimental works and all my friends who were aware and took my concern to heart throughout my SUT student life.

The most importantly, my genuine gratitude to my dearest family for their strong encouragement, belief, love and support during my study period.

Ei Ei San

TABLE OF CONTENTS

	Page
ABSTRACT (THAI).....	I
ABSTRACT (ENGLISH).....	II
ACKNOWLEDGEMENTS.....	IV
TABLE OF CONTENTS.....	V
LIST OF TABLES.....	VIII
LIST OF FIGURES.....	X
SYMBOLS AND ABBREVIATIONS.....	XIII
CHAPTER	
I INTRODUCTION.....	1
1.1 Background and rationale.....	1
1.2 Research objectives.....	2
1.3 Scope and limitations.....	2
1.4 Research methodology.....	3
1.4.1 Literature review.....	3
1.4.2 Sample collection and preparation.....	5
1.4.3 Laboratory testing.....	5
1.4.4 Analysis and Comparison.....	6
1.4.5 Computer simulations.....	6
1.4.6 Discussions and Conclusions.....	6

TABLE OF CONTENTS (Continued)

	Page
1.4.7 Thesis Writing.....	6
1.5 Expected results.....	7
1.6 Thesis contents.....	7
II LITERATUREREVIEW.....	8
2.1 Literature review.....	8
2.2 Underground mining and subsidence.....	8
2.3 Sealing materials and their properties.....	9
2.4 Laboratory tests.....	15
2.5 Numerical simulations.....	19
III SAMPLE PREPARATION.....	25
3.1 Introduction.....	25
3.2 Materials.....	25
3.2.1 Cement (C) and sugarcane bagasse ash (SCBA).....	25
3.2.2 Bentonite and crushed salt.....	27
3.2.3 Saturated brine.....	28
3.3 Sample preparation.....	28
IV LABORATORY TESTING.....	33
4.1 Introduction.....	33
4.2 Laboratory test.....	33
4.2.1 X-ray fluorescence method.....	33
4.2.2 Porosity test.....	35

TABLE OF CONTENTS (Continued)

	Page
4.2.3 Uniaxial compressive strength (UCS) test.....	38
4.2.4 Brazilian tensile strength (BZ) test.....	43
4.2.5 Triaxial compression (TRI) test.....	44
V COMPUTER SIMULATION.....	51
5.1 Introduction.....	51
5.2 Related studies and input parameters.....	51
5.3 Simulation results.....	58
VI DISCUSSIONS, CONCLUSIONS AND RECOMMENDATION	
FOR FUTURES STUDIES.....	61
6.1 Discussions and conclusions.....	61
6.3 Recommendations for future studies.....	65
REFERENCES.....	66
APPENDIX A SUMMARIZES DIMENSIONS OF THE SPECIMEN.....	73
BIOGRAPHY.....	80

LIST OF TABLES

Table		Page
3.1	Chemical compositions of C and SCBA.....	26
4.1	WDXRF results for four raw materials.....	35
4.2	WDXRF results for CPB mixtures.....	35
4.3	Porosity and void ratio of CPB mixtures at each curing period.....	37
4.4	Uniaxial compressive strength of CPB-1 and CPB-2 mixtures.....	39
4.5	Elastic modulus, E and Poisson's ratio, ν of CPB-1 and CPB-2 mixtures.....	40
4.6	Brazilian tensile strength of CPB-1 and CPB-2 mixtures.....	43
4.7	Normal stress (σ_1) and confining pressure (σ_3) of CPB-1 mixture.....	48
4.8	Normal stress (σ_1) and confining pressure (σ_3) of CPB-2 mixture.....	48
4.9	Cohesion and internal friction angle of CPB mixtures at each curing Period.....	50
5.1	Visco-elastic and visco-plastic properties of rock salt for FLAC 4.0 simulations (Samsri et al., 2010).....	57
5.2	Mechanical properties of clastic rock and of rock salt for FLAC 4.0 simulations (Crosby, 2007; Sriapai et al., 2012).....	57
5.3	Mechanical properties of CPB mixtures for FLAC 4.0 simulations.....	57
5.4	Subsidence reduction with the function of sealing time.....	59
A.1	Specimen dimensions of CPB-1 mixture for Porosity test.....	74

LIST OF TABLES (Continued)

Table		Page
A.2	Specimen dimensions of CPB-2 mixture for Porosity test.....	74
A.3	Specimen dimensions of CPB-1 mixture for UCS test.....	75
A.4	Specimen dimensions of CPB-2 mixture for UCS test.....	75
A.5	Specimen dimensions of CPB-1 mixture for BZ test.....	76
A.6	Specimen dimensions of CPB-2 mixture for BZ test.....	77
A.7	Specimen dimensions of CPB-1 mixture for TRI test.....	78
A.8	Specimen dimensions of CPB-2 mixture for TRI test.....	79

LIST OF FIGURES

Figure	Page
1.1 Research methodology.....	4
2.1 Typical salt creep behavior showing the three major transient strain phases in response to constant stress (Goodman, 1989).....	23
2.2 Volumetric strain and brine flow as function of time (Hansen, 1997).....	24
3.1 The sulphate resistant Portland cement (ASTM Type V) sample.....	26
3.2 Sugarcane bagasse ash (SCBA) sample.....	26
3.3 Bentonite sample.....	27
3.4 Crushed salt sample.....	27
3.5 Saturated brine.....	28
3.6 The professional 600™ series 6-Quart stand mixer.....	29
3.7 Summary of CPB mixtures preparation.....	29
3.8 Samples of PVC molds with 53 – 56 mm diameters.....	30
3.9 Sample preparation by using diamond saw.....	31
3.10 Examples of sealing materials before and after the Uniaxial compressive strength (UCS) test.....	31
3.11 Examples of sealing materials before and after the Triaxial compression (TRI) test.....	32

LIST OF FIGURES (Continued)

Figure	Page
3.12 Examples of sealing materials before and after the Brazilian tensile strength (BZ) test.....	32
4.1 Summary of WDXRF test procedure.....	34
4.2 Porosity test machine.....	36
4.3 Porosity, n and void ratio, e for both CPB mixtures.....	37
4.4 Uniaxial compressive strength (UCS) test.....	38
4.5 UCS values for both CPB mixtures at 3, 7, 14 and 28 days.....	39
4.6 Elastic modulus, E and Poisson's ratio, ν for CPB mixtures at 3, 7, 14 and 28 days.....	40
4.7 Stress-Strain curves for UCS tests of CPB-1 at 3, 7, 14 and 28 days.....	41
4.8 Stress-Strain curves for UCS tests of CPB-2 at 3, 7, 14 and 28 days.....	42
4.9 Brazilian tensile strength (BZ) test.....	43
4.10 Brazilian tensile strength of CPB-1 and CPB-2 mixtures.....	44
4.11 Triaxial compression (TRI) test.....	45
4.12 Stress-Strain curves for TRI tests of CPB-1 at 3, 7, 14 and 28 days.....	46
4.13 Stress-Strain curves for TRI tests of CPB-2 at 3, 7, 14 and 28 days.....	47
4.14 The strength development of CPB mixture with curing period.....	48
4.15 Cohesion and Internal friction angle of CPB mixtures with curing period.....	49
5.1 Stratigraphy of borehole no. K-089 at Ban Hhao, Muang district, Udon Thani province (Suwanich et al., 1986).....	52

LIST OF FIGURES (Continued)

Figure		Page
5.2	The modular components and their output result from the time-dependent analysis of the Burgers model (Goodman, 1989).....	53
5.3	Vertical distribution of the different salt layers at Bamnet Narong, Chaiyaphum Province (Hansen et al., 2016).....	55
5.4	Mesh boundary conditions used in this study.....	56
5.5	Surface subsidence as a function of time with overturn thickness = 250 m and opening height = 10 m.....	59

SYMBOLS AND ABBREVIATIONS

C	=	cement
SCBA	=	Sugarcane bagasse ash
CPB	=	Cemented paste backfill
CPB-1	=	Mixture with 1:2 composition ratios of cementitious materials to bentonite-crushed salt
CPB-2	=	Mixture with 1:3 composition ratios of cementitious materials to bentonite-crushed salt
UCS	=	Uniaxial compressive strength test,
TRI	=	Triaxial compression strength test
BZ	=	Brazilian tensile strength test
SG	=	Specific gravity
n	=	porosity
e	=	Void ratio
V_v	=	Volume of voids in the sample
V_s	=	Volume of solid in the sample
V	=	Total volume of the sample
σ_c	=	Uniaxial compressive strength
P	=	Failure load
A	=	Cross-sectional area of the tested sample
σ	=	Triaxial compression strength
σ_1	=	Total failure stress

SYMBOLS AND ABBREVIATIONS (Continued)

σ_3	=	Confining stress
σ_t	=	Brazilian or splitting tensile strength
L	=	Thickness of the specimen
D	=	Diameter of the specimen
ρ	=	Density
c	=	Cohesion
ϕ	=	Friction angle
E	=	Elastic modulus
ν	=	Poisson's ratio
$\epsilon_1(t)$	=	Axial strain with time
K	=	Bulk modulus
G_2	=	Elastic shear modulus
G_1	=	Constants used in Equation (5.1)
η_1	=	Constants used in Equation (5.1)

CHAPTER I

INTRODUCTION

1.1 Background and rationale

Underground mining creates voids in different shapes which evoke the environmental impact such as subsidence that leads the collapse of the upper strata and the foremost effect to engineering structures and natural resources. These underground voids should, therefore, be sealed with backfill materials to diminish the subsidence effects, prolong mine stability and facilitate future excavation. Among the different types of backfill, the use of cemented paste backfill (CPB) can provide better safety factor for underground mining environments. Many industrial by-products have been incorporated as supplementary cementing materials to exhibit more unique characteristics than ordinary CPB. Sugarcane Bagasse Ash (SCBA), an agro-industrial by-product of the sugar mills, has recently been used as cement replacement material to reduce the cost, huge energy consumption and carbon dioxide (CO₂) emission from cement production. It is mainly composed of silica and other high amounts of aluminum, iron and calcium oxides that can provide the better results in cement reaction. This study will concentrate on the strength development of SCBA mixtures with increasing curing times to use as sealant materials alongside with reduction in subsidence in salt and potash mine. Their time-dependent behaviors will also be simulated by using numerical simulations.

1.2 Research objectives

The objectives of this study are the suitability of the utilization of SCBA as 20% cement replacement material in the mixture of SCBA, cement, bentonite and crushed salt, and its efficiency on subsidence reduction in salt and potash mine. Towards this, the uniaxial compressive strength (UCS) test, triaxial compression (TRI) test and Brazilian tensile strength (BZ) test are carried out for each curing period of 3, 7, 14 and 28 days to determine the strength and toughness development of that mixture to use as cemented paste backfill. The test results are used in FLAC program to simulate the time dependent behaviors of salt and potash mine with sealing materials.

1.3 Scope and limitations

The scope and limitations of this study are as followed.

1. Four materials will be used.
 - 1.1 Portland Cement (Type V, High Sulfate Resistance)
 - 1.2 Sugarcane Bagasse Ash (SCBA) from Mitr Phol Phu Luang mill in Leoi Province, Thailand.
 - 1.3 Bentonites
 - 1.4 Crushed salt from the Lower members of the Maha Sarakham Formation in the Korat basin, northeastern Thailand.
2. The mix ratio of cementitious materials to bentonite – crushed salt mixture will be 1:2 and 1:3 in which SCBA is 20% replacement of cement and bentonite to crushed salt will be 30:70 percent by weight.

3. Saturated brine will be used to compose mixture and the ratio of saturated brine to solid materials will be 0.4.
4. The samples will be cylindrical shapes with 53 - 56 mm diameters.
5. Uniaxial compressive strength test, triaxial compression test and Brazilian tensile strength test will be performed in accordance with ASTM standards and FLAC Program will be used for numerical modelling.
6. The confining pressures for triaxial test will be 100, 200, 300 and 400 psi (0.69, 1.28, 2.07 and 2.76 MPa).
7. The four levels of curing periods will be 3, 7, 14 and 28 days.

1.4 Research methodology

The research methodology shown in Figure 1.1 encloses with six steps consisting of literature review, sample collection and preparation, laboratory testing including uniaxial compressive strength test, triaxial compression test and Brazilian or splitting tensile strength test, analysis and comparison, computer simulations, discussion and conclusion, and thesis writing.

1.4.1 Literature review

Literature review will be emphasized to study the previous researches related with the application of SCBA and required properties to use as a sealing material in mining. The sources of information for this research are associated with standard specifications, journals, technical reports and conference papers. A summary of literature review will be shown in the thesis.

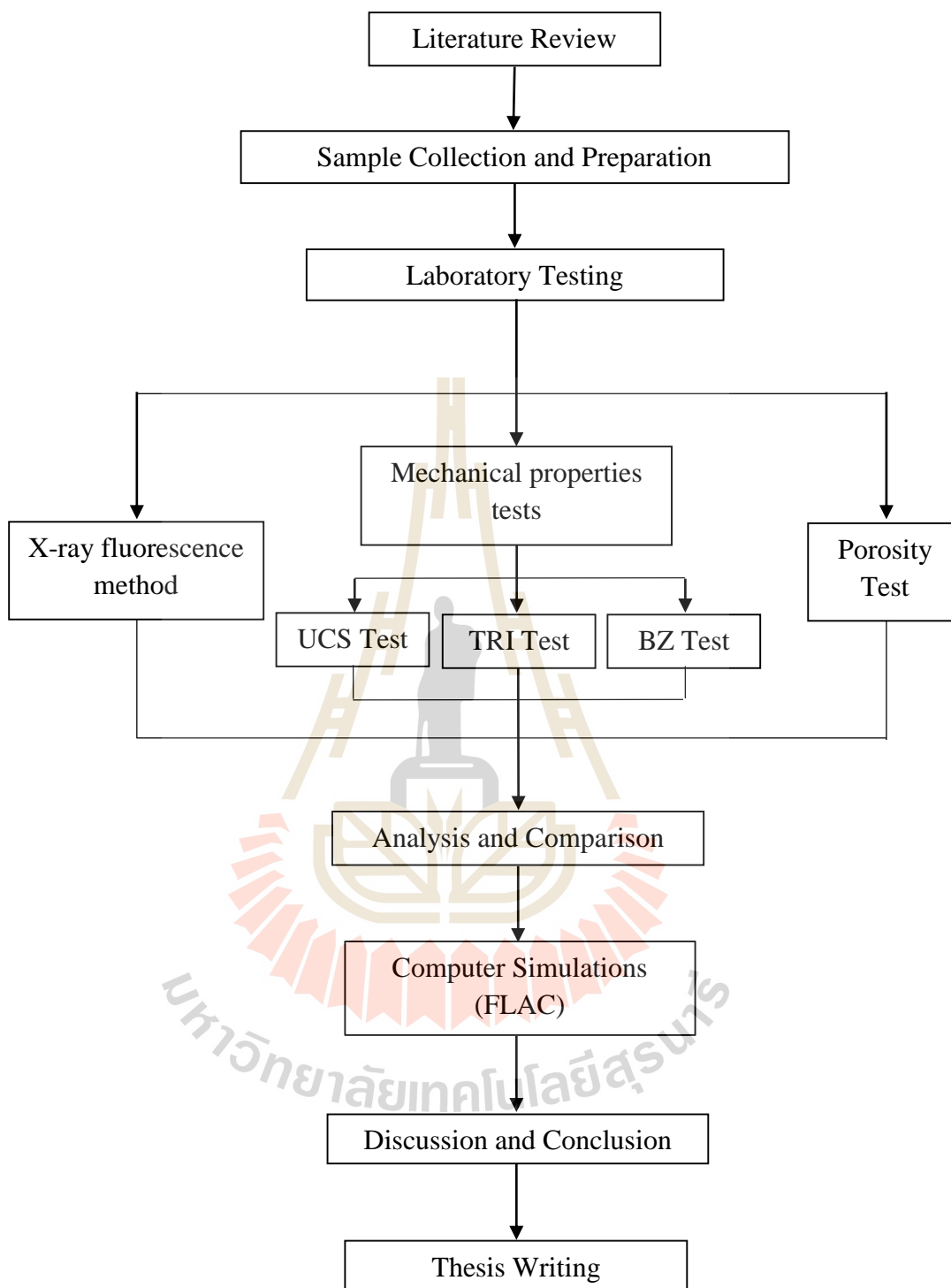


Figure 1.1 Research methodology.

1.4.2 Sample collection and preparation

The tested samples for this research will be mixed with four materials. These materials, firstly, will be weighed and mixed thoroughly with the relevant ratios. That mixture will then be mixed with saturated brine to mixture ratio of 0.4 by using mixer machine to become the paste form. That paste will be placed into the 53 - 55 mm diameter PVC mold and cured for 3, 7, 14 and 28 days. Engineering properties of all materials are suggested by ASTM standards and all tests will be carried out in the Geomechanics Research laboratory of Suranaree University of Technology.

1.4.3 Laboratory testing

Laboratory testing will consist of X-ray fluorescence method to determine the chemical properties, porosity test for physical properties and three mechanical properties tests; uniaxial compressive strength test, triaxial compression test and Brazilian tensile strength test. These tests will be performed for each curing period of 3, 7, 14 and 28 days. In mechanical properties tests, the loading will be applied from 20-ton hydraulic load cell connected to the hydraulic hand pump until failure occurs and the maximum applied load at failure point will be measured by pressure gages. For triaxial compression test, confining pressures of 0.69, 1.28, 2.07 and 2.76 MPa will be used. The axial and lateral displacements will be recorded by high precision dial gages. These values will be used to determine the compressive and splitting tensile strength, elastic modulus (E), Poisson's ratio (ν), cohesion (c) and friction angle (ϕ).

1.4.4 Analysis and comparison

The results from three mechanical properties tests for both mixtures will be illustrated in the graphs and tables to interpret the variations of strength, elastic modulus, Poisson's ratio, cohesion and friction angle at four curing periods of 3, 7, 14 and 28 days. The maximum strength values of each mixture will be selected to use in the FLAC program.

1.4.5 Computer simulations

Finite difference method (FLAC 4.0) will be used to analyze the specific time dependent movements of the model used in this research. The specifications for the model will be defined according to the results of laboratory tests and calculations. The time to seal in mine will also be considered as the suggested CPB mixtures for this research can be prepared and placed right after the mine process.

1.4.6 Discussions and conclusions

The comparison of the results of the laboratory and computer simulation, research activities and methods will be adapted in the discussion and conclusions.

1.4.7 Thesis writing

All research preparation, methods and results will be documented and conceded in the thesis. This research aims the use of the sugarcane bagasse ash mixture as sealing material can effectively reduce the surface subsidence in salt and potash mines. The results of this research will be presented at an international conference or journal.

1.5 Expected results

This research will disclose the strength development and time-dependent behavior of the sugarcane bagasse ash mixture as the cemented paste backfill with elapsed time to use as a sealing material for underground mining. Furthermore, SCBA used in this research will be intended as an eligible cement substitute for construction.

1.6 Thesis contents

Chapter I describes the objectives, rationale, and methodology of the research. **Chapter II** summarizes results of the literature review on the properties of all the proposed four materials, laboratory testing and numerical simulations. **Chapter III** describes the sample preparation and **chapter IV** presents the laboratory testing and their results. **Chapter V** shows the result of surface subsidence calculated from computer simulation (FLAC program). Discussions, conclusions and recommendations for future research needs are given in **Chapter VI**.

CHAPTER II

LITERATURE REVIEW

2.1 Introduction

This chapter summarizes the relevant background of underground mining and subsidence, and previous theoretical research of sealing materials, ASTM standards of the laboratory tests and computer modeling. The reviewing theory and background knowledge of sealing materials enhance to understand the laboratory tests and practical applications.

2.2 Underground mining and subsidence

Underground mining is the extraction of natural resources underneath the ground surface and already popular in mine organizations because it has general appearance without large slope and can provide high production rate due to no effect of weather condition. However, it needs high energy consumption and constant maintenance for the safety of operators.

The extraction of natural resources from the ground generally creates large underground voids. The range of these underground voids depends on the magnitude of the in-situ stresses, mining induced stresses, immediate roof characteristics and presence of geological discontinuities. With time, the superjacent strata moves into the voids, resulting in instability of underground workings and forms a depression on the ground surface which is commonly referred to as a subsidence, an undeniable

consequence of the underground mining, and the foremost effect to engineering structures. In the worst cases, it can cause injury or loss of life (Sahua et al., 2015).

At first, surface subsidence may be small and confined but after many years, it extends gradually over large areas. It can generally implicate both vertical and lateral ground movements. Although rock properties and geological structures greatly impact the surface subsidence, its intensity counts on a number of factors as diverse as extraction height, mining depth and method, panel dimensions, overlying strata properties, geological disturbances, surface topography and more (Ju et al., 2015).

These underground voids in mine should therefore, be backfilled with the waste materials to ensure regional stability, minimize ore dilution, control subsidence, facilitate subsequent excavation and provide a stable platform for the workers and ground support for the nearby regions (Sivakugan et al., 2015).

2.3 Sealing materials and their properties

Backfilling has different techniques that have been successfully implemented in mine filling worldwide. Some of well-known techniques that have been used in practice are mechanical backfill, pneumatic backfill, Hydraulic backfill and paste backfill.

Among these different types of backfills, the use of cemented paste backfill (CPB) becomes an increasingly important component and standard practice for use in underground mining operations (Landriault et al., 1997 and Naylor et al., 1997). It ultimately improves the productivity because of ground support to the pillars and walls, and prevention of caving and roof falls to enhance pillar recovery (Belem et al., 2004).

Cement is a significant building material used in almost every construction because it has good plasticity, workability and good moisture-resistance to provide strength and stiffens the building structure. For the durability of the building structure, the composition of mortar and concrete becomes the main factor to consider.

In the preparation of mortar and concrete, water is often added in the mixtures for easy workability. The additional mixing water can help easy mixing and workability but it may increase porosity. Apparently the more porous the mortar or concrete, the weaker it will be. Many experiments indicate that the most important source of porosity in mortar or concrete is the ratio of water to cement, known as the water-cement (w/c) ratio. Because a change in the w/c ratio affects the compressive strength of a cement mortar or concrete more than their flexural or tensile strengths.

Schulze (1999) states that the compressive strength of both modified and unmodified mortars depends on water-cement (w/c) ratio and, to a lesser extent, on the cement content of the mortars. Compressive strength is decreased with increasing w/c ratio but the flexural strength is nearly independent of w/c ratio and cement content at w/c ratio of 0.4 – 0.6.

Singh et al. (2015) studied the effect of water-cement (w/c) ratio on the mechanical properties such as compressive strength and split tensile strength of cement mortar cylinders and cubes for 28 days curing period. The research included the various proportions of cement to river sand such as 1:3, 1:4, 1:5, 1:6, 1:7, 1:8 with different w/c ratios. Results shown that compressive strength and split tensile strength of cement mortar decreased with an increase in the w/c ratio. They concluded that the

minimum w/c ratio required to make the cement mortar workable is 0.5 with 1:3 cement to sand proportion.

In the concrete, higher water-cement (w/c) ratio can better actuate hydration. But the consumed water for hydration reaction in cement paste develops to more pores which lead to reduction of not only strength but also durability. Yun-Yong et al. (2014) considered the effect of w/c ratio on durability and porosity of cement mortar by using constant cement amount. In early aged state, porosity shows relatively rapid reduction due to hydration and it later generally decreases with age in curing condition. With increasing w/c ratio from 0.45 to 0.60, porosity goes up to 150% and compressive strength is reduced to 75.6%. Although they have the same cement amount, 33% additional water causes considerable changes in the performances.

Naik (1997) states that the presence of capillary pores, air voids created by water particles movements or space not occupied by solid components, influences the permeability of concrete to a large extent. Permeability of concrete increases with the increase in porosity of concrete which decreases concrete density. For achieving high durability, concrete porosity should be kept low so as to reduce its permeability.

Accordingly the concrete durability is affected by the different facts such as a number of parameters, including water to cementitious materials ratio, degree of hydration, air content, consolidation, admixtures, aggregates, reaction between aggregate and the hydrated cement paste, mixture proportioning, etc. Among these facts, the introduction of pozzolanic materials, such as fly ash, natural pozzolans, slags, rice husk ash, and silica fume causes refinement of grain and pore structures in the production of high-strength concretes.

In recent years, a variety of industrial by-products and agricultural wastes have been incorporated as supplementary cementing materials in formulating CPBs in the mining industry to cover an increasing demand and consumption of cement and in the backdrop of problems associated with environmental, technical and waste management. This utilization can not only increase product performance and technical benefits but also reduce cement content resulting in reduced carbon emission and, therefore, supporting sustainable development. The materials incorporating supplementary cementing materials exhibit unique characteristics that often make them more durable than ordinary CPBs (Tariq et al., 2013).

Many researches had shown that waste materials have a significant amount of amorphous silica in their chemical composition which can be used as pozzolanic materials and increased strength in mortar or concrete. When these materials are mixed with cement, the presented silica reacts with the free lime from the hydration of the cement and new silicate hydrate products are formed, that can improve the compressive strength, pore structure, and permeability of the mortars and concretes because the total porosity decreases with increasing the hydration time (Ganesan et al., 2007).

There are many industrial by-products and agricultural wastes such as fly ash, rice husk ash, wheat straw ash, hazel nutshell and sugarcane bagasse ash that have been used as pozzolanic materials for the development of blended cements. Out of all these materials, sugarcane bagasse ash (SCBA) is selected as a cement replacement material for this study.

Cordeiro et al. (2008) and Balaji (2015) have a look on the utilization of the waste material such as sugarcane bagasse ash (SCBA) can be advantageously used as

a replacement of cement in the preparation of concrete because of its pozzolanic effects. SCBA is a combustion by-product of the sugar mills and alcohol factories. Composed mainly of silica and other high amounts of un-burnt matter, aluminum, iron and calcium oxides, this agro-industrial by-product can be advantageously used as a mineral admixture in mortar and concrete.

Ganesan et al. (2007) studied the effects of SCBA content as partial replacement of cement on physical and mechanical properties of hardened concrete. The properties of concrete investigation included compressive strength, splitting tensile strength, water absorption, permeability characteristics, chloride diffusion and resistance to chloride ion penetration. The test results indicated that SCBA is an effective mineral admixture, with 20% as optimal replacement ratio of cement.

Idris et al. (2015) investigated the physical properties and chemical composition of SCBA as well as compressive strength properties of the mortar produced by 5, 10, 15, 20 and 30 percentages by weight of replacement Portland clinker with bagasse ash. The results showed that SCBA is a good pozzolan with combined SiO_2 , Al_2O_3 and Fe_2O_3 of 78.12% and 10% SCBA substitution is adequate to gain maximum benefit of strength.

According to the study of Amin (2011), SCBA is an effective mineral admixture with the optimal replacement ratio of up to 20% cement without any adverse effect on the desirable properties of concrete. The specific advantages of such replacement are the development of high early strength, reduction in water permeability, and appreciable resistance to chloride permeation and diffusion.

Another ideal grout material for sealing or backfilling into the borehole or water-resistant barriers, bentonite, has been widely used because it has low

permeability, proper swelling capacity, sorptive and self-sealing behaviors. Domitrovic et al., 2013 states that the colloidal particle sizes in bentonites attract molecules of water and that causes increase in volume several times, and it plays an important part in the mechanical properties including strength, deformability and hydraulic conductivity.

Mikkelsen (2002) describes the installations of single-component solid bentonite sealing products are usually difficult to place successfully and time consuming, particularly on deeper boreholes or casing. And they are sensitive to over-mixing, difficult to pump down the small diameter grout pipes, and cannot stable volumetrically and introduce pore water pressures caused by the hydration process. To make a stable grout, cement or fly ash can be mixed with bentonite to reduce its expansive properties and adjust the variations in temperature, pH and cleanliness of the water.

Fuenkajorn and Daemen (1987) studied the mechanical relationship between cement, bentonite and surrounding rock. The study included the mechanical interaction between multiple plugs and surrounding rock and identification of potential failure. Results from the experiment indicate that the sufficient mechanical stability of bentonite seal can be obtained when the sealing is done below groundwater level and the mechanical stability of sealing in hard rock is higher than in soft rock.

Kelsall et al. (1984) suggest crushed salt as a major backfill component in schematic designs of penetration seal for salt repositories. Creep closure of the storage room, tunnels, and shafts is likely to compress the crushed salt backfill and

create an impermeable monolith to retard ground water flow and radionuclide migration.

Case and Kelsall (1987) examined the potential of crushed salt for required sealing access shafts and drifts in long-term periods. They investigated crushed salt backfill as a potential backfill and seal material through laboratory testing to determine how fundamental properties such as permeability, porosity and creep rate are reduced by pressure and time through consolidation. All the tests were performed at ambient temperature and confining pressures ranging from 0.34 MPa to 17 MPa. The most significant result from the tests was the influence of moisture on permeability, porosity and volumetric creep strain rate. In addition, the consolidation rate for the moist sample was more rapid at comparable porosities.

Butcher et al. (1991) consider a mixture of 70% by weight salt and 30% by weight bentonite as sealant for disposal rooms in the Waste Isolation Pilot Plant. Because less bentonite will isolate in individual pores and reduce its effectiveness for wicking brine from other regions of the backfill. But more bentonite will reduce the quasi-static rigidity within the mixture and increase the cost of the backfill. They conclude that 30% bentonite filler is about the smallest portion that assures its continuous paths throughout the mixture and the real advantage of the salt/bentonite backfill depends on bentonite's potential for absorbing brine and radionuclides.

2.4 Laboratory tests

In designing of cement used buildings and other structures, the compressive strength test is the most common preferable test for the engineer. The reason is concrete is usually brittle in tension but relatively tough in compression so the

compressive strength is typically much higher than the tensile strength. The uniaxial compressive strength (UCS) is used as an index property in many design formula since deformation and strength are the functions of loading conditions.

ASTM (D7012-14) determines the compressive strength under uniaxial compression. In this method, the deformation states are monitored while applying the axial load continuously until the load becomes constant. The maximum resulted load by the specimen is recorded to find the uniaxial compressive strength. The uniaxial compressive strength, σ_c of the test specimen can be calculated by using equation (2.1):

$$\sigma_c = P/A \quad (2.1)$$

where σ_c is the uniaxial compressive strength (MPa), P is the failure load (kN) and A is cross-sectional area of the tested sample (mm²).

In the triaxial compression strength test, the predetermined confining pressure is applied uniformly to the specimen until the failure mode is detected. The triaxial compressive strength, σ in this test can be obtained by using equation (2.2):

$$\sigma = \sigma_1 - \sigma_3 \quad (2.2)$$

where σ is triaxial compressive strength, σ_1 is the total failure stress and σ_3 is the confining stress. The unit of all of these stresses are MPa. However, the strength values determined in this method are only in terms of total stress and are not corrected for pore pressure.

Arioglu et al. (1995) recognize that the uniaxial stress-strain relationship is influenced by the detailed information regarding the effects of the size and shape of tested specimen, characteristics of the test machine, type of strain measurement and properties of the concrete including strength, water/cement ratio, cement content, mechanical properties of the coarse aggregate used and aggregate volume concentration, and curing conditions and age.

Mier et al. (1997) report that the strength of concrete under uniaxial compression test is depended on the slenderness of the specimen and the type of used loading platen. Their tests prove that with decreasing slenderness and increase of specimen strength measured by using friction-reducing measure, the stress-strain curve indicates a more ductile behavior.

When a concrete structure is under extreme loadings, the material is subjected to high triaxial compressive stresses. In order to provide high stress level with well-controlled loading paths, static triaxial tests are carried out on concrete samples with a very high-capacity triaxial press. The confining pressure is applied on every surfaces of the sample through the membranes until the desired pressure is reached.

Vu et al. (2009, 2011) show that during the deviatoric phase of behavior, regardless of the w/c ratio of concrete, the confinement can very sharply raise both the ductility and the loading capacity of the concrete. A drop in w/c ratio increases the confinement level which corresponds to the brittle-ductile behavior transition and reduces cement concentration effect on concrete strength.

At high confinement level, furthermore, concrete behaves like a non-cohesive granular stacking, and the cement concentration has little effect on concrete deviatoric behavior and leads to increase concrete axial tangent stiffness. These results feature

that increasing confinement level is likely to reduce the cement concentration in concretes for the purpose of raising their strength capacity to contend extreme loadings.

Yurtdas et al. (2004a) highlighted the influence of drying and desiccation shrinkage on mechanical uniaxial behavior of a standard mortar. Through numerous uniaxial compression tests with loading-unloading cycles under various conditions, 20% is increased in mortar strength and about 10 and 25 % decrease in elastic modulus and Poisson's ratio with the loss in mass respectively. These are the result of capillary depression generated by drying as well as the micro-cracking created by exceeding tensile strength. Thus, tensile strength has to be taken into account in modeling of the coupling between desiccation and mechanical behavior of concrete.

When concrete is subjected to tensile forces, it develops cracks because of its brittle nature. For this reason, the determination of the concrete's tensile strength is necessary to measure the load at which the concrete may crack with respect to the appearance and durability. However, the tensile test is difficult and expensive for typical application.

Splitting tensile strength test is a well-known indirect method to find the tensile strength of concrete which is one of the basic and important properties. This test is also known as Brazilian Test because it was first proposed by Lobo Carneiro and Barcellos during the Fifth Conference of the Brazilian Association for Standardization in 1943.

ASTM (D3967-08) is usually used to determine the splitting tensile strength by diametric line compression. It appears as a desirable alternative method of tensile test because it is much simpler and inexpensive. It is also one of the simplest tests to

represent the complicated field conditions where various combinations of compressive and tensile stresses are occurred. According to this method, splitting tensile strength, σ_t can be calculated from the equation (2.3):

$$\sigma_t = 2P / \pi LD \quad (2.3)$$

where σ_t is splitting tensile strength (MPa), P is the maximum applied load (kN), L is the thickness of the specimen (mm) and D is the diameter of the specimen (mm).

The main interest of the splitting test is that it requires only external compressive loads. A cylindrical specimen is placed horizontally and compressed along two diametrically opposed generators to induce a nearly uniform tensile stress in the loading plane. To prevent local failure in compression at the loading generators, two thin strips, usually made of plywood, are placed between the loading platens and the specimen to distribute the load. The induced tensile stress state causes the specimen to fail by splitting. The maximum value of the tensile stress, computed at failure from the theory of elasticity, is the splitting tensile strength.

2.5 Numerical simulations

FLAC (Itasca, 2002), a two-dimensional explicit finite difference program, has been primarily developed for geotechnical engineering applications in the field of mining, underground engineering, rock mechanics and research. This program stimulates the analysis of progressive failure and collapse of structures built of soil, rock or other materials that may undergo plastic flow when their yield limits are reached.

Materials are represented by elements or zones, which form a grid that is adjusted by the user to fit the shape of the object to be modeled. Each element behaves according to a prescribed linear or nonlinear stress/strain law in response to the applied forces or boundary restraints. The material can yield and flow and the grid can deform (in large-strain mode) and move with the material that is represented. The explicit, Lagrangian calculation scheme and the mixed discretization zoning technique used in FLAC ensure that plastic collapse and flow are modeled very accurately.

The drawbacks of the explicit formulation (i.e., small time step limitation and the question of required damping) are overcome to some extent by automatic inertia scaling and automatic damping that do not influence the mode of failure. Moreover, FLAC contains a powerful built-in programming language, FISH, which enables to define new variables and functions with great flexibility in designing models for complex material behavior representation.

Malan (1999) also describes that time-dependent behavior is an important factor in every engineering applications because it is a general deformation related with non-elastic-dynamic behavior and geometric changes in the dimensions of an excavation, and occurs on a time scale of days to years. In his study, the author used the time-dependent closure data in deep level tabular excavations to deduce the rock mass behavior and stress in the fracture zone and to identify hazardous conditions such as areas prone to face bursting. He also used two-dimensional plain strain version of FLAC program using built-in FISH languages for his developed elastic-viscoplastic model.

Duncan et al. (1993) state that deep and high extraction mining is possible only through management of rock mass failure. Generally, the failure may occur in

two modes – ductile and brittle. Ductile failure consumes sufficient energy to prevent its acceleration, or at least enough energy to remove any hazard to miners. That is, the failure process will be sufficiently slow to give miners time to retreat. The alternative is sudden and hazardous brittle failure. The unexpected transition from a controlled ground failure process to a brittle failure process can bring many fatal accidents and mine disasters.

Minkley et al. (1996) studied many collapses during mining of carnallite potash seams. Generally, the lower the halite content of a rock (with carnallite replacing halite) the more brittle its behavior. Initiation of collapse is generally attributed to a blasting event that begins a chain-reaction failure incorporating both pillars and roof strata, resulting in significant surface subsidence and a large seismic event. The ground subsidence area was bounded by an inferred fault or shear zones. These faults and shear zones apparently weakened the overburden, about 200 meters above the mining level. Injection of wastewater into this and adjacent dolomite strata may have devoted to weakening of these features. Generally soft strata were associated with slow development of a subsidence trough while the presence of stronger strata was related with sudden subsidence events. Failure of strong strata was found to occur on near-vertical shears.

Malevichko et al. (2005) describe the potash as “almost incompressible, highly ductile and rather easily deformed by creep.” In their work, potash was extracted from two to three beds with 10 to 16 m of total extraction height in the Mines of the Verkhnekamskoye Potash Deposit. The mine was used a panel system of rooms and pillars under 200 to 400 m of overburden. Rooms were 13-16 m wide and pillars 11-14 m wide by 200 m long. Surface subsidence typically reached 50% of excavation

height 4- 8 months after excavation. This event occurred 15 years after mining began, and 7 years after mining was completed. The unusual delay in subsidence implies extensive bridging of overburden, consistent with its uncommonly high release of seismic energy.

When the excavations are started in salt mining, the damage of rock and disturbance begins to occur because of the stress change. It then extends a shorter distance into the rock, represented by large deviatoric stresses, leading to salt dilatation, which includes existing apertures opening and creation of new micro- and macro-fractures. At this state, salt undergoes transient inelastic deformation, where the strains continue to change with time under constant stress. This transient behavior is commonly referred to as creep, or the stress-strain constitutive relation under such conditions (Kuhlman and Malama, 2013).

Li et al. (2015) state that surface subsidence of salt caverns is influenced by several factors including depth, internal pressure, geological and operating conditions. Because of the good creep properties of rock salt, lower rock salt layer under hydrostatic pressure state is able to maintain long-term stability. However, this balance is broken in the mining zone, and the processes of stress redistribution and creep deformation will take place. During this processes, the volume of the cavern is reduced and transferred upwards through the overburden layers, and spreads to the surface to form the final surface subsidence.

Typical salt creep behavior is illustrated in Figure 2.1 where the three commonly observed phases of the transient strain curve are depicted schematically. It comprises the instantaneous elastic response and the short-term inelastic response

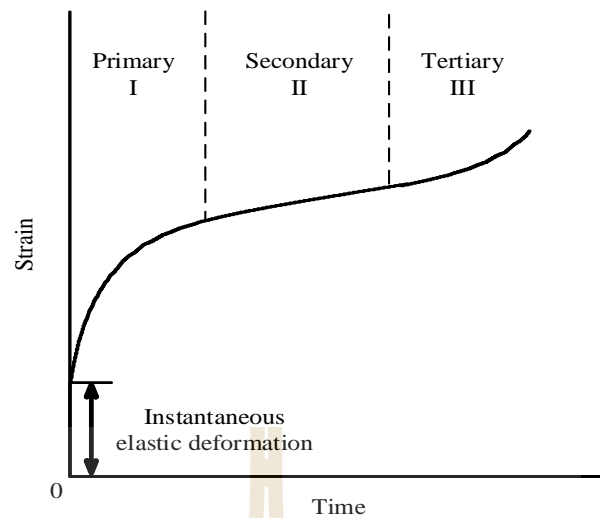


Figure 2.1 Typical salt creep behavior showing the three major transient strain phases in response to constant stress (Goodman, 1989).

consisting of a nonlinear primary phase, a linear secondary (also referred to as steady-state creep) phase and a nonlinear tertiary phase which is rapidly followed by failure.

Brine can easily displace gas in multi-phase flow if the gas is not trapped. Therefore, brine flow towards a borehole or excavation in salt which is usually accompanied by surface subsidence is fundamentally a multi-phase (multicomponent) process because salt deforms, creeps, and heals under relevant repository conditions. Figure 2.2 shows the relationship between the volumetric strain and brine flow as function of time. In conclusion, creep or time-dependent behavior is essential factor in salt and potash mines.

The Department of mineral Resources, Thailand studied the nature of salt and potash in northeastern Thailand by comparing the total boreholes which had been drilled as many as 194 drill holes from 1973 to 1982. And they figured out that rock strata of Maha Sarakham Formation is mostly composed of rock salt and can be

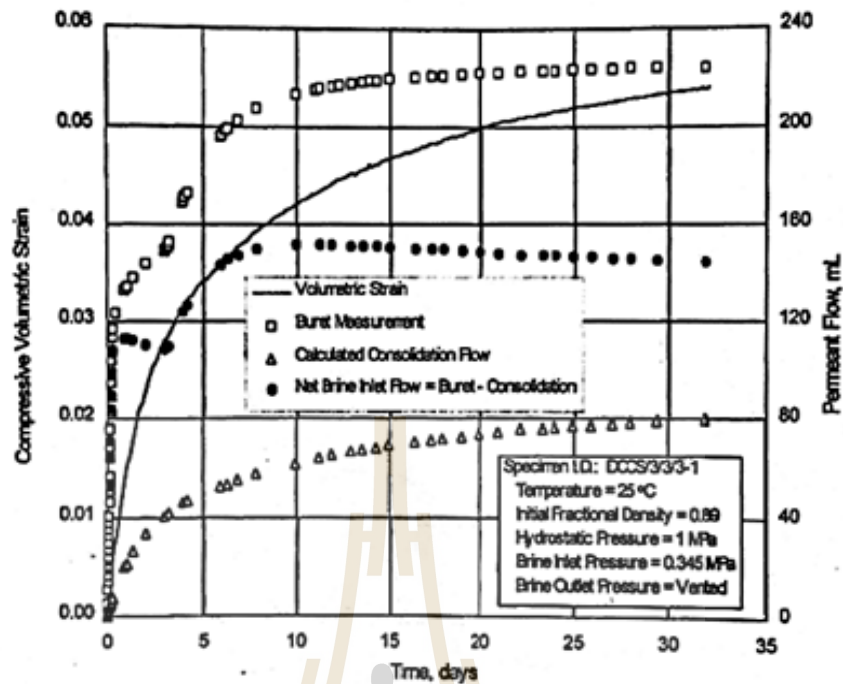


Figure 2.2 Volumetric strain and brine flow as function of time (Hansen, 1997).

divided under the overburden or top soil as, Upper Clastic, Upper salt, Middle Clastic, Middle salt, Lower Clastic, Coloured Salt, Potash Zone, Lower Salt, Basal Anhydrite and some minor other layers. This data should be noted in computer simulations because the properties of overburden also take an important role in the determination of deformation state of sealing materials.

CHAPTER III

SAMPLE PREPARATION

3.1 Introduction

This chapter describes the basic characteristics and preparation of materials used in this study. The four materials are used in the laboratory testing. They are sugarcane bagasse ash (SCBA), cement, bentonite, and crushed salt.

3.2 Materials

3.2.1 Cement (C) and sugarcane bagasse ash (SCBA)

The sulphate resistant Portland cement, C (Type V according to ASTM C150/C150M (2016e1)) is used in this study (Figure 3.1). SCBA is collected from Mitr Phol Phu Luang mill in Leoi Province, Thailand. Before sample preparation, SCBA is kept in a hot-air oven at 100°C for at least 24 hours to reduce the moisture content. And then it is sieved through the mesh number 40 (sieve opening 0.42 mm) to obtain grain size ranging from 0.001 to 0.475 mm (Figure 3.2). The chemical compositions for C and SCBA are determined using X-ray fluorescence method and compared in Table 3.1. In this method, silica contents in SCBA is emphasized to prove its capability as pozzolanic material. The results clearly show that silica contents in SCBA is three times higher than that of C. At that time, CaO content is noticeably different; only 3% in SCBA but C has about 51% and also considerable difference in sulphate content (0.72% in SCBA and 4.02% in C). All other chemicals of SCBA are less than those in C except MgO and Na₂O.



Figure 3.1 The sulphate resistant Portland cement (ASTM Type V) sample.

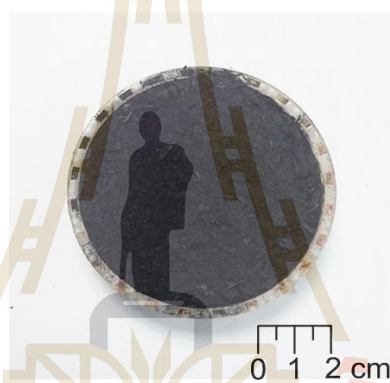


Figure 3.2 Sugarcane bagasse ash (SCBA) sample.

Table 3.1 Chemical compositions of C and SCBA.

Chemical compositions	Concentration (% by weight)	
	C	SCBA
SiO ₂	24.14	76.82
Al ₂ O ₃	7.66	6.25
Fe ₂ O ₃	10.01	6.28
CaO	51.03	2.78
MgO	1.41	1.99
Na ₂ O	0.98	1.91
K ₂ O	0.75	3.25
SO ₃	4.02	0.72

3.2.2 Bentonite and crushed salt

Bentonites, ideal grout materials for sealing or backfilling into the borehole or water-resistant barriers, are applied into the mixture because it has low permeability, proper swelling capacity, sorptive and self-sealing behaviors (Figure 3.3). Crushed salts (Figure 3.4) are used as coarse-grained materials in this study and prepared from the Lower member of the Maha Sarakham formation in the Korat basin, northeastern Thailand. The grain sizes of crushed salt are ranged from 0.075 to 2.35 mm by passing through sieve number 4, 8, 18, 40, 60, 100, 140 and 200. The openings are 4.75, 2.36, 1, 0.425, 0.25, 0.15, 0.106 and 0.075 mm, respectively.

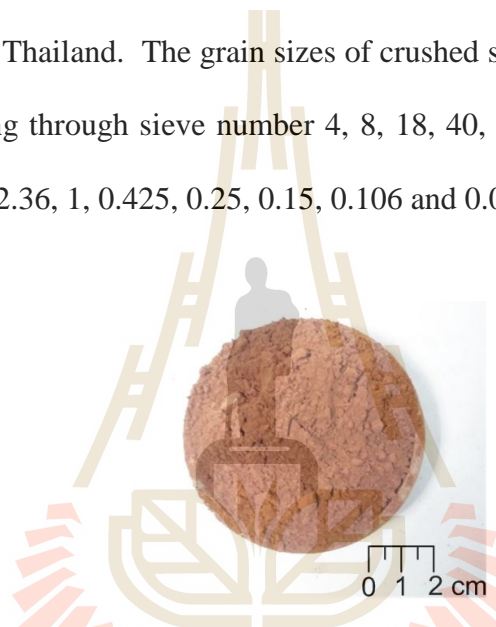


Figure 3.3 Bentonite sample.

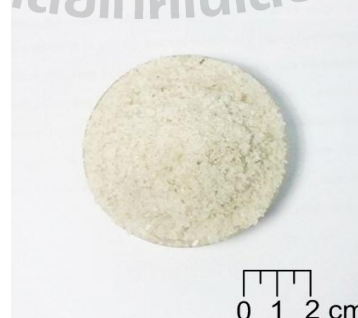


Figure 3.4 Crushed salt sample.

3.2.3 Saturated brine

Saturated brine (Figure 3.5) is prepared from pure salt (NaCl) of 2.7 kg dissolved with distilled water in plastic tank and stirred by a plastic stick continuously for 20 minutes. The proportion of salt and water is more than 39% by weight. The specific gravity of saturated brine can be calculated by $SG_{\text{Brine}} = \rho_{\text{Brine}}/\rho_{\text{H}_2\text{O}}$, where SG_{Brine} is specific gravity of saturated brine, ρ_{Brine} is density of saturated brine (measured with a hydrometer (kg/m^3)) and $\rho_{\text{H}_2\text{O}}$ is density of water (kg/m^3) equal $1,000 \text{ kg}/\text{m}^3$. The SG of the saturated brine in this study is 1.211 at 21°C .

3.3 Sample preparation

The four materials are mixed according to their weight ratios. At first, cementitious materials are prepared by replacing C with 20% of SCBA in dry condition. And then the ratio of bentonite to crushed salt with 30:70 is used (Butcher et al., 1991). These two mixtures are then mixed with 1:2 and 1:3 composition ratios of cementitious materials to bentonite-crushed salt to form the final mixture. The ratio of saturated brine to mixture materials is fixed at 0.4.

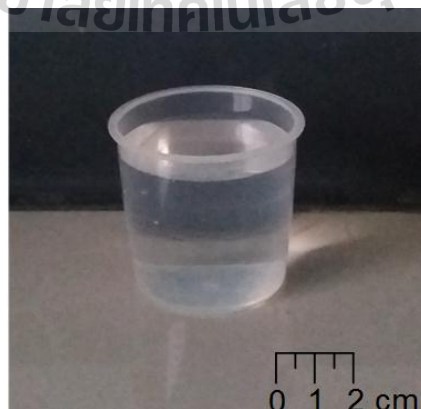


Figure 3.5 Saturated brine.

The CPB mixtures are prepared using the professional 600™series 6-Quart stand mixer (Figure 3.6) for a total of three minutes. Figure 3.7 shows the summary of CPB mixtures preparation. After thoroughly mixed, the CPB mixtures were poured into the 53-56 mm diameter PVC mold (Figure 3.8). The molds were then sealed and cured for periods of 3, 7, 14 and 28 days.



Figure 3.6 The professional 600™series 6-Quart stand mixer.

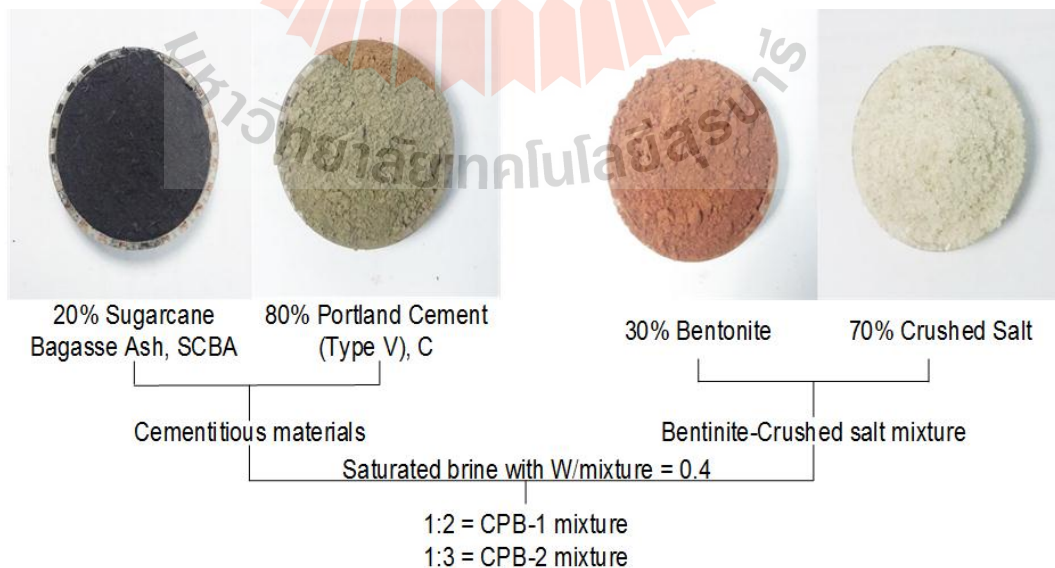


Figure 3.7 Summary of CPB mixtures preparation.

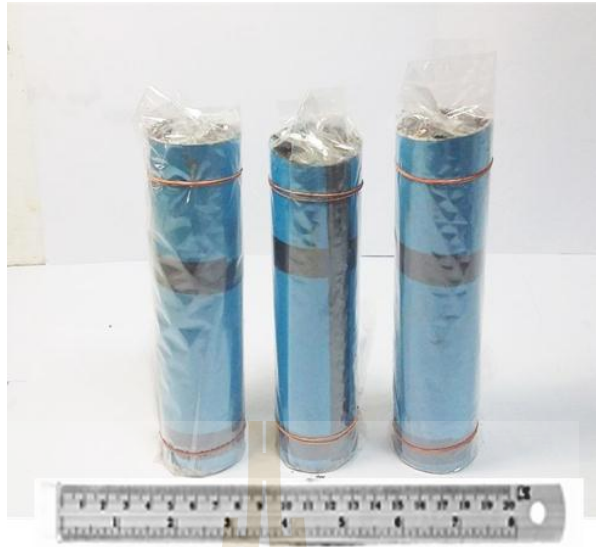


Figure 3.8 Samples of PVC molds with 53 – 56 mm diameters.

The specimens are then cut with relevant length to diameter ratio (L/D) (Figure 3.9). For UCS test, three specimens with L/D of 2.5 were prepared for both mixtures. Another four specimens with L/D ratio of 2 for TRI test and ten specimens with 0.5 L/D for BZ test are also prepared to determine the mechanical strengths of CPB mixtures after curing. Some of the examples of sealing material after curing in PVC mold prepared for laboratory test are shown in Figure 3.10 to 3.12.



Figure 3.9 Sample preparation by using diamond saw.



Figure 3.10 Examples of sealing materials before and after the uniaxial compressive strength (UCS) test.



Figure 3.11 Examples of sealing materials before and after the triaxial compression (TRI) test.

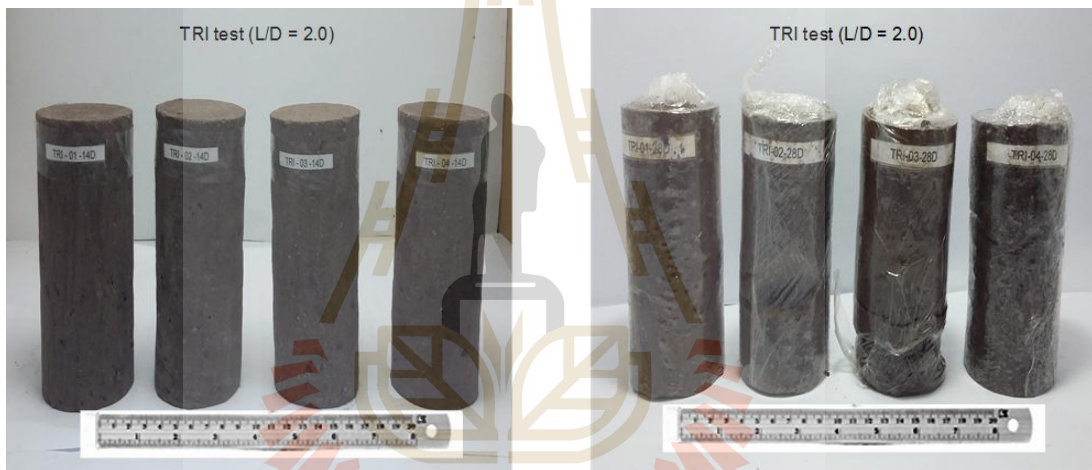


Figure 3.12 Examples of sealing materials before and after the Brazilian tensile strength (BZ) test.

CHAPTER IV

LABORATORY TESTING

4.1 Introduction

This chapter describes the test methods and their results obtained from the laboratory experiments to determine the chemical, physical and mechanical properties of CPB mixtures.

4.2 Laboratory test

There are three types of laboratory tests in this study. Firstly, X-ray fluorescence method is used to determine the chemical properties of CPB mixtures and porosity test is used for physical properties. Then mechanical properties are determined by using uniaxial compressive strength (UCS) test, triaxial compression (TRI) test and Brazilian tensile strength (BZ) test at each curing period of 3, 7, 14 and 28 days.

4.2.1 X-ray fluorescence method

In this study, Wavelength Dispersive X-ray fluorescence Spectrometry (WDXRF) method is used to analyze the changes in chemical properties of CPB mixtures at each curing period. All the used materials in this method including four raw materials and CPB mixtures are powder type. At first, 3 grams of powder-typed materials are mixed with 7 grams of microcrystalline binder respectively. That mixture is then put under compressor by applying 150 kN load for 2 minutes. The

resulted compressed powder is then placed inside the WDXRF machine and run to determine the chemical compositions. Figure 4.1 shows the procedure for this test.

In this method, nine chemical compounds are determined and the output chemical composition data are summarized in Table 4.1 for four raw materials and Table 4.2 for CPB mixtures at each curing period of 3, 7 and 30 days. Out of all those compositions after reaction with brine, MgO, Al₂O₃, SiO₂, Cl and CaO are slightly increased in early states but then tend to decrease for both mixtures and reversely; Na₂O and K₂O are gradually decreased in their first week and increased later. At that time, Fe₂O₃ is steadily decreased with increasing sulphate content in both CPB mixtures.

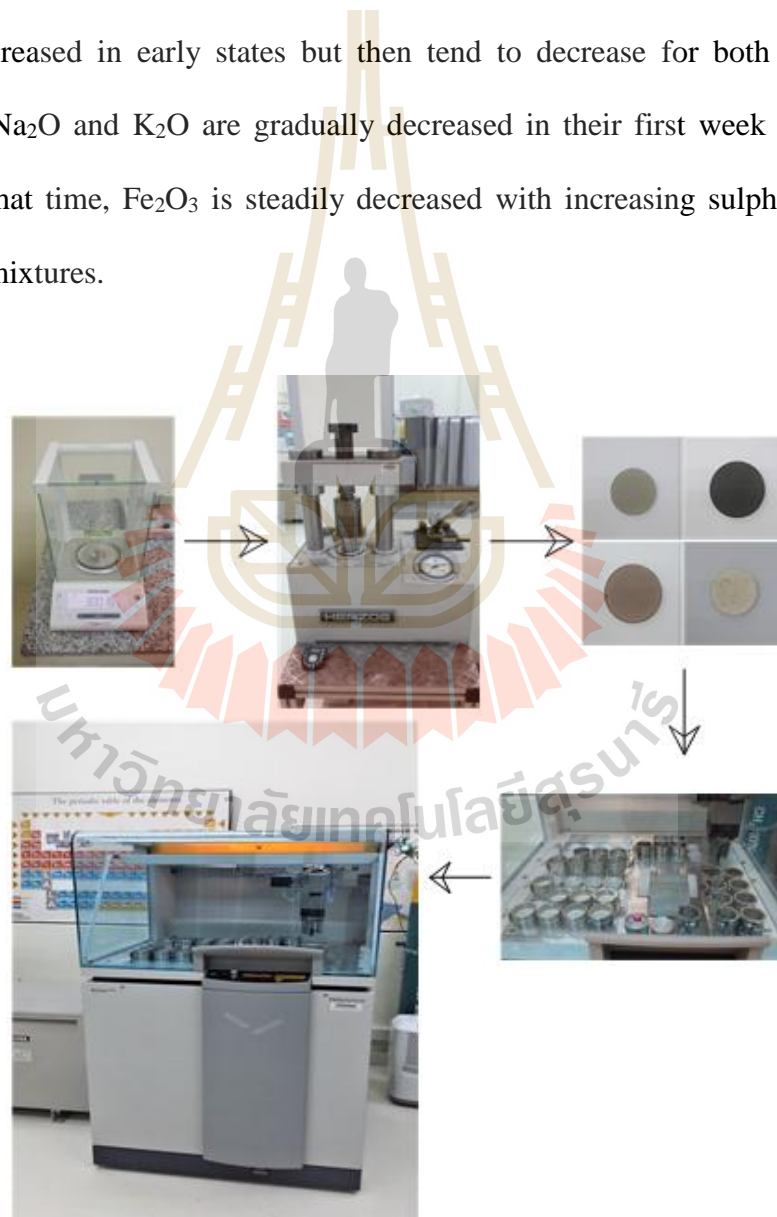


Figure 4.1 Summary of WDXRF test procedure.

Table 4.1 WDXRF results for four raw materials.

% by weight	C	SCBA	Bentonite	Crushed Salt
Na ₂ O	2.039	0.563	5.308	34.553
MgO	1.687	2.169	4.348	2.348
Al ₂ O ₃	10.156	8.864	19.182	5.254
SiO ₂	26.893	78.292	52.675	13.012
SO ₃	3.736	0.478	0.135	3.377
Cl	0.106	0.339	0.134	36.132
K ₂ O	0.947	3.185	0.859	0.659
CaO	47.151	2.273	4.277	4.345
Fe ₂ O ₃	7.284	3.837	13.081	0.321

Table 4.2 WDXRF results for CPB mixtures.

% by weight	CPB-1			CPB-2		
	3D	7D	30D	3D	7D	30D
Na ₂ O	26.143	24.611	28.56	25.312	26.427	26.937
MgO	0.852	0.895	0.806	0.705	0.866	0.657
Al ₂ O ₃	4.089	4.335	3.793	3.244	3.802	3.172
SiO ₂	12.600	13.791	13.132	10.019	11.779	10.152
SO ₃	1.147	1.343	1.415	0.944	1.184	1.075
Cl	33.274	33.780	31.883	37.785	36.401	39.345
K ₂ O	0.708	0.647	0.780	0.685	0.615	0.821
CaO	13.714	13.732	14.333	13.435	11.541	11.338
Fe ₂ O ₃	7.474	6.866	5.298	7.871	7.384	6.504

4.2.2 Porosity test

The state of the porosity can influence permeability, flowability and durability of paste, mortar and concrete. Especially porosity determines the rates at which aggressive species can enter the mass and cause disruption. More importantly,

it is related to the mechanical properties of cementitious materials. In this study, porosity is determined in terms of helium diffusion (Figure 4.2).

Porosity, n and void ratio, e are calculated using the following relation (Das, 2010):

$$n = V_v / V_n \quad (4.1)$$

$$e = V_v / V_s \quad (4.2)$$

where n is the porosity (%), e is the void ratio (%), V_v is the volume of voids in the sample (cm^3), V_s is the volume of solid in the sample (cm^3) and V is the total volume of the sample (cm^3). The results obtained from this study are described in Figure 4.3 and summarized in Table 4.3.



Figure 4.2 Porosity test machine.

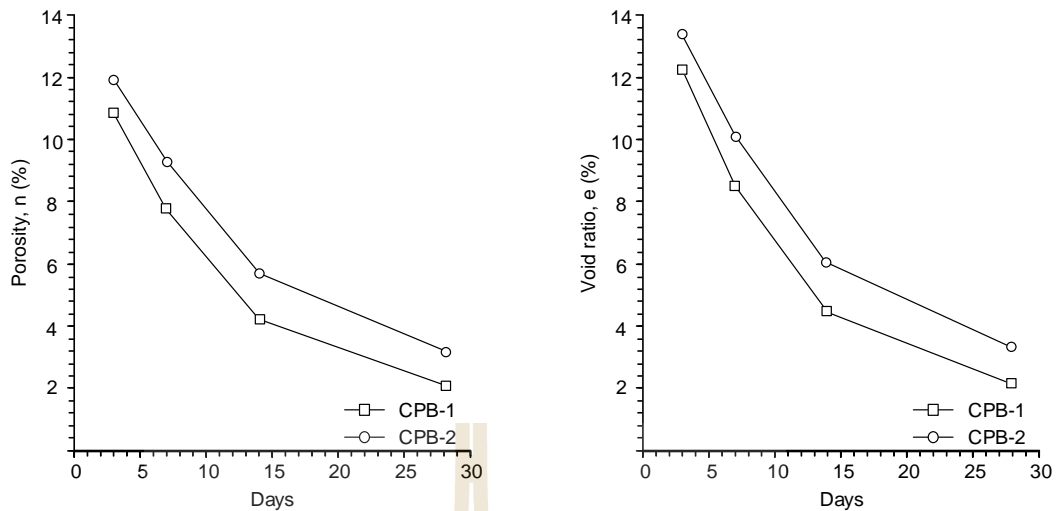


Figure 4.3 Porosity, n and void ratio, e for both CPB mixtures.

Table 4.3 Porosity and void ratio of CPB mixtures at each curing period.

Curing time (Days)	Porosity, n (%)		Void Ratio, e (%)	
	CPB-1	CPB-2	CPB-1	CPB-2
3	10.90	12.23	11.94	13.56
7	7.84	8.51	9.35	10.31
14	4.28	4.47	5.77	6.12
28	2.13	2.18	3.26	3.37

It can be clearly seen that the trends of porosity and void ratio are descending for both CPB mixtures with time. Their values are gradually decreased; the 28-day porosity of CPB-1 mixture is about 20% less than that of 3-day result (from 10.90% to 2.13%). At that time, the ratios of voids are decreased from over 12% at 3 days to only 2% at 28 days.

Similarly, porosity of CPB-2 mixture is reduced from 11.94% porosity at 3 days to 3.26% at 28 days (about 27%) and nearly 14% 3-day void ratio is loss to 3.37% at 28 days. Even though the decreasing rate of porosity and void ratios of both

CPB mixtures is similar, the reduction values of CPB-1 mixture are more than that of CPB-2 mixture. According to the porosity test, it can be considered that CPB-1 mixture is more useable than CPB-2 mixture.

4.2.3 Uniaxial compressive strength (UCS) test

This UCS test is carried out by applying axial load from hydraulic hand pump until the failure occurs (ASTM D7012-14). Two dial gages are installed longitudinally to determine the axial deformation and other two are placed laterally at the mid-height of specimen for lateral deformation as shown in Figure 4.4. These values are monitored until failure occurs. The maximum applied load at the failure and failure modes are recorded.

The results described in Table 4.4 and Figure 4.5 clearly show that the UCSs of both mixtures are gradually increased with the curing periods and 28-day UCS values are over the minimum requirement of 5 MPa. Three-day UCS values of CPB-1 mixture is equivalent to the 7-day UCS values of CPB-2 mixture, whereas

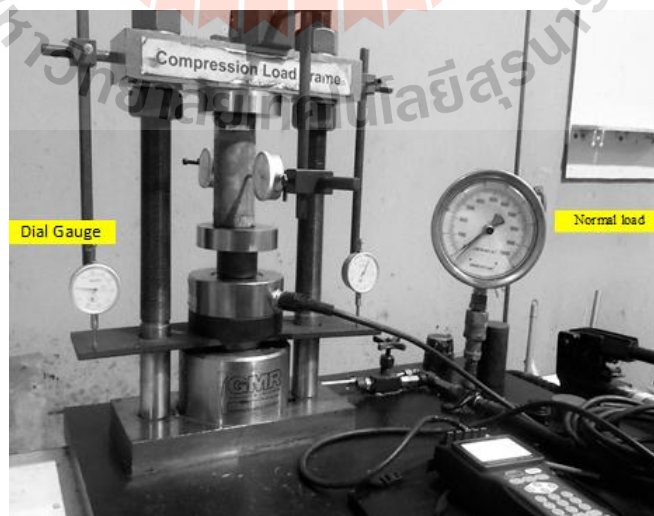
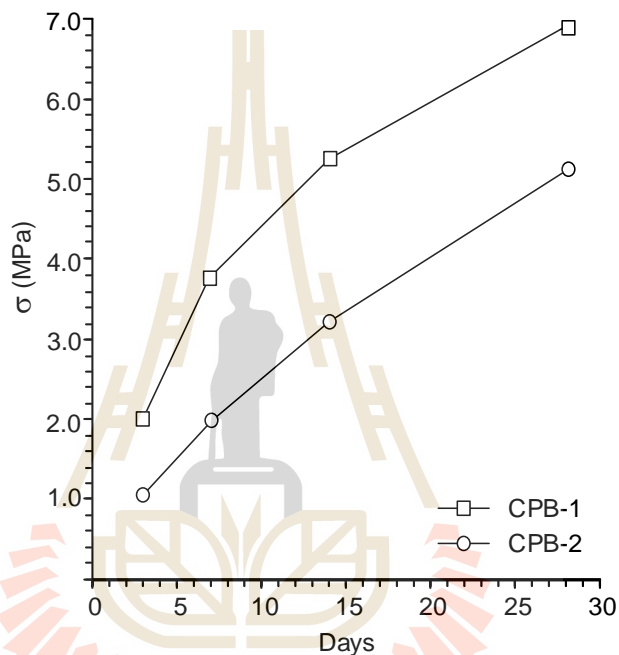


Figure 4.4 Uniaxial compressive strength (UCS) test.

Table 4.4 Uniaxial compressive strength of CPB-1 and CPB-2 mixtures.

Mixture	Uniaxial compressive strength (MPa)			
	3 days	7 days	14 days	28 days
CPB-1	2.01	3.76	5.19	6.87
CPB-2	1.08	2.01	3.22	5.12

**Figure 4.5** UCS values for both CPB mixtures at 3, 7, 14 and 28 days.

other values of CPB-1 mixture are higher than CPB-2 mixture. When CPB-2 mixture provides 5.12 MPa at 28 days, CPB-1 mixture can support 5.19 MPa at only 14 days.

The calculated elastic moduli and Poisson's ratio from UCS test are summarized in Table 4.5. In Figure 4.6, the behaviors of the elastic moduli and Poisson's ratio related with time are described. According to the figure, all the trends are slightly increased with time. Although the elastic moduli of CPB-1 mixture are greater than CPB-2 mixture, the values of Poisson's ratio are lesser. Therefore, the

use of CPB-1 mixture is more effective and can provide more strength than that of CPB-2 mixture. The recorded UCS values of both CPB-1 and CPB-2 mixtures are also shown in Figure 4.7 and 4.8.

Table 4.5 Elastic modulus, E and Poisson's ratio, ν of CPB-1 and CPB-2 mixtures.

Curing time (Days)	Elastic modulus, E (MPa)		Poisson's ratio, ν	
	CPB-1	CPB-2	CPB-1	CPB-2
3	4.005	2.143	0.09	0.19
7	5.703	2.961	0.12	0.21
14	7.384	5.295	0.17	0.25
28	11.002	8.081	0.22	0.30

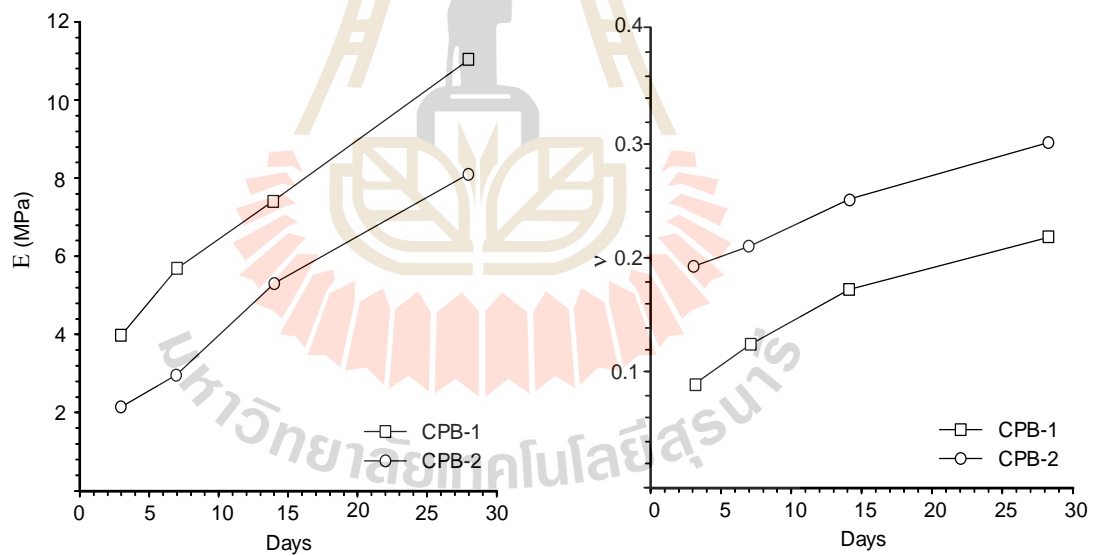


Figure 4.6 Elastic modulus, E and Poisson's ratio, ν for CPB mixtures at 3, 7, 14 and 28 days.

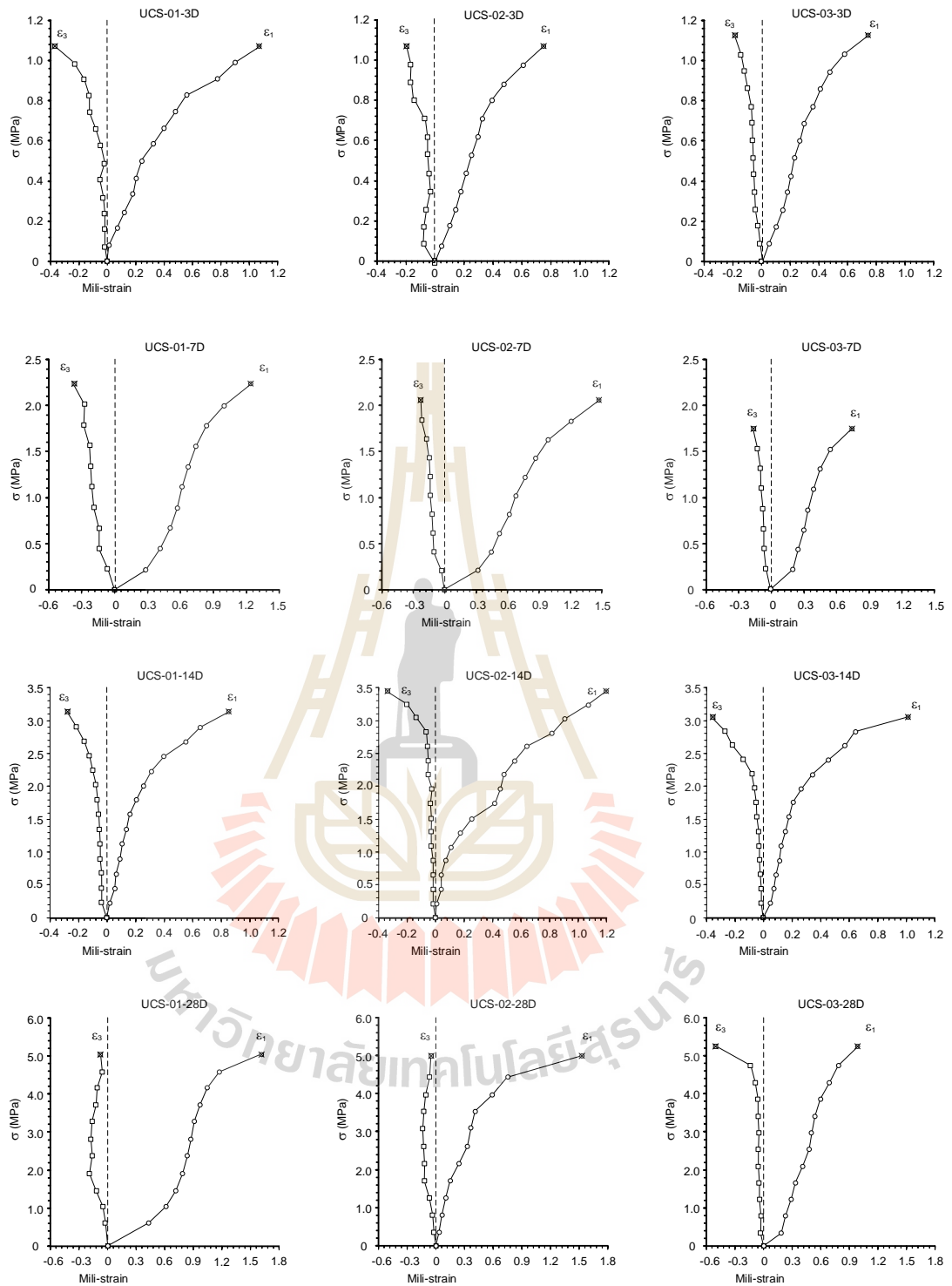


Figure 4.7 Stress-Strain curves for UCS tests of CPB-1 at 3, 7, 14 and 28 days.

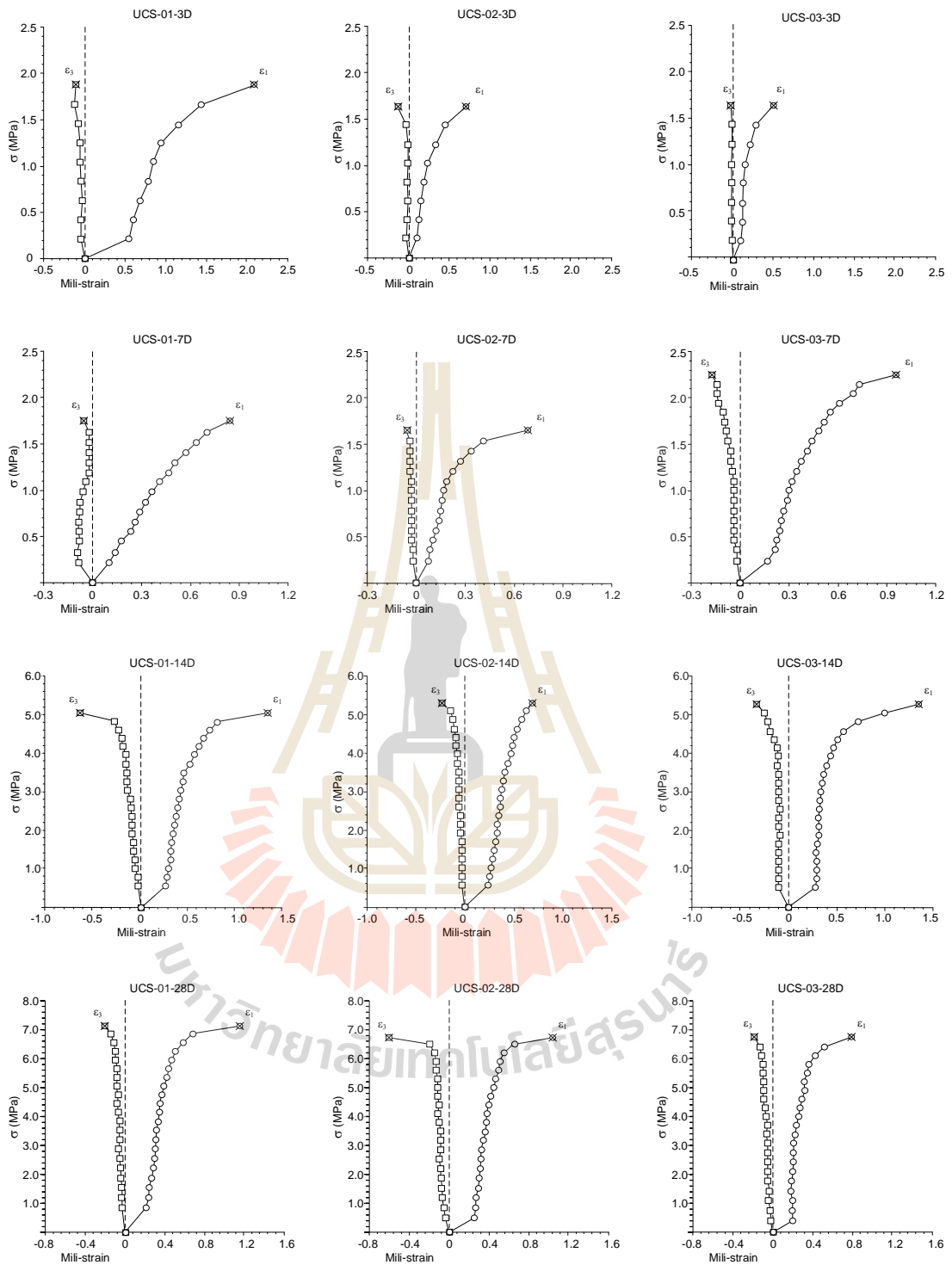


Figure 4.8 Stress-Strain curves for UCS tests of CPB-2 at 3, 7, 14 and 28 days.

4.2.4 Brazilian tensile strength (BZ) test

In this indirect method, the specimen is placed diametrically (ASTM D3967-08). The loading will be steadily increased by pressing the hydraulic hand pump until failure occurs (Figure 4.9). Table 4.6 and Figure 4.10 show the increasing tensile strength values of CPB-1 and CPB-2 mixtures at each curing periods. The results show that the strength values of 14-day CPB-1 mixture is similar with 28-day strength values of CPB-2 mixture. Obviously CPB-1 mixture is also more useful than CPB-2 mixture from the tensile strength point of view.

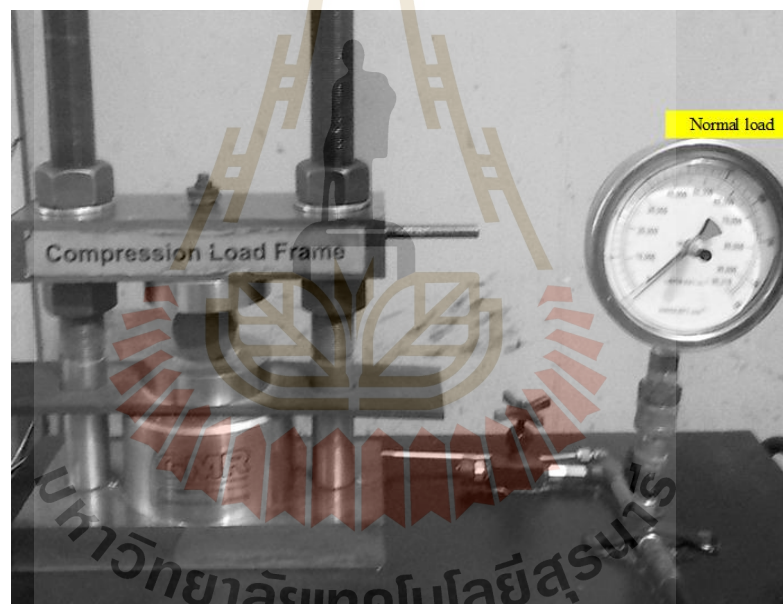


Figure 4.9 Brazilian tensile strength (BZ) test.

Table 4.6 Brazilian tensile strength of CPB-1 and CPB-2 mixtures.

Mixture	Brazilian tensile strength (MPa)			
	3 days	7 days	14 days	28 days
CPB-1	0.519	0.663	0.838	1.115
CPB-2	0.238	0.351	0.547	0.859

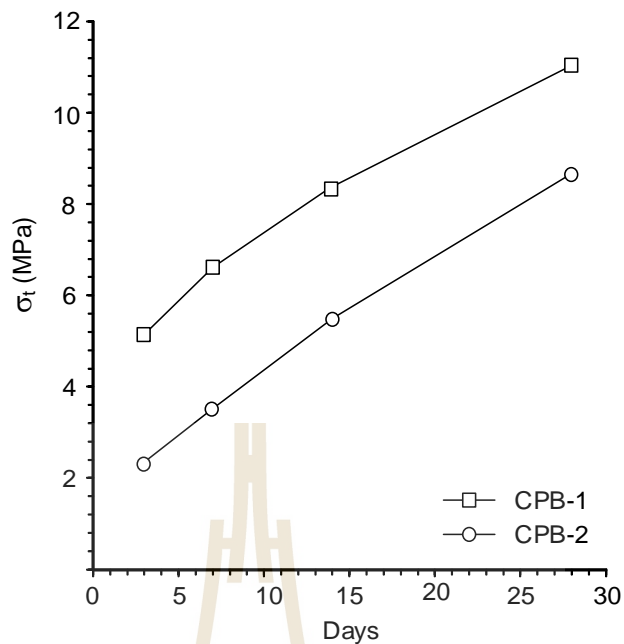


Figure 4.10 Brazilian tensile strength of CPB-1 and CPB-2 mixtures.

4.2.5 Triaxial compression (TRI) test

For this test, the prepared specimen is placed in the Hoek cell and applied the confining pressure by increasing from 0.69, 1.28, 2.07, to 2.76 MPa (ASTM D7012-14). That Hoek cell and two longitudinal dial gages are set up in the loading machine and the pipette is installed at the outlet valves to find the oil level which later transform into volumetric deformation (Figure 4.11).

Axial load is increased constantly on the specimen by pressing the hydraulic hand pump until failure occurs. While the axial load is increasing, the value of confining pressure is made sure to be constant by controlling the valves. The failure load is recorded to simulate the strength and failure criteria. Figure 4.12 and 4.13 show the resulted values of both CPB mixtures at each curing period.

The relationship between normal stress (σ_1) and confining pressure (σ_3) of 0.69, 1.28, 2.07, and 2.76 MPa for CPB mixtures are shown in Figure 4.14. The values are summarized in Table 4.7 for CPB-1 mixture, and Table 4.8 for CPB-2 mixture. The strength results of both mixtures are steadily increased with curing time. Although the trends of increasing strength for both mixtures are similar, the graphs show that the 28-day strength of CPB-2 mixture with confining pressures of 2.76 MPa is 70.78 MPa which is nearly equal to the CPB-1 mixture with only confining pressures of 0.69 MPa.

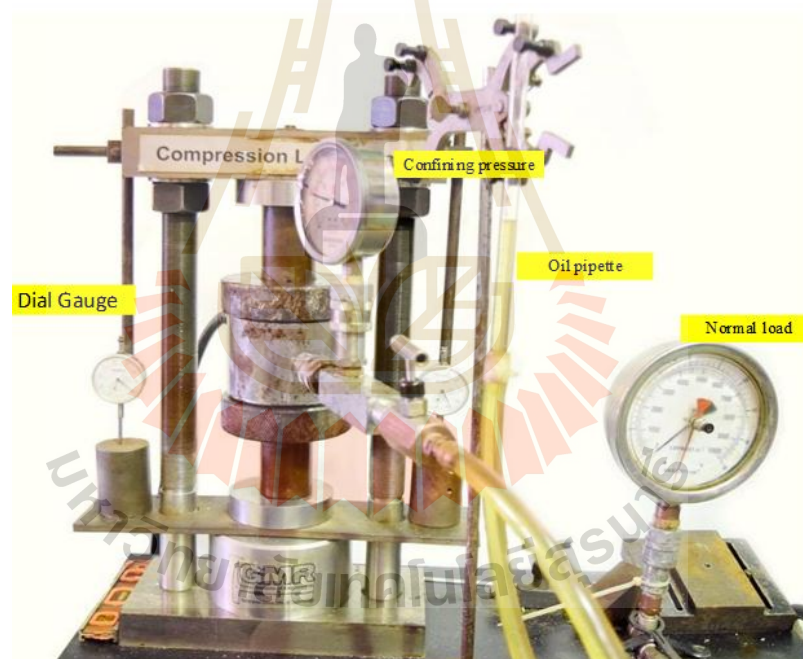


Figure 4.11 Triaxial compression (TRI) test.

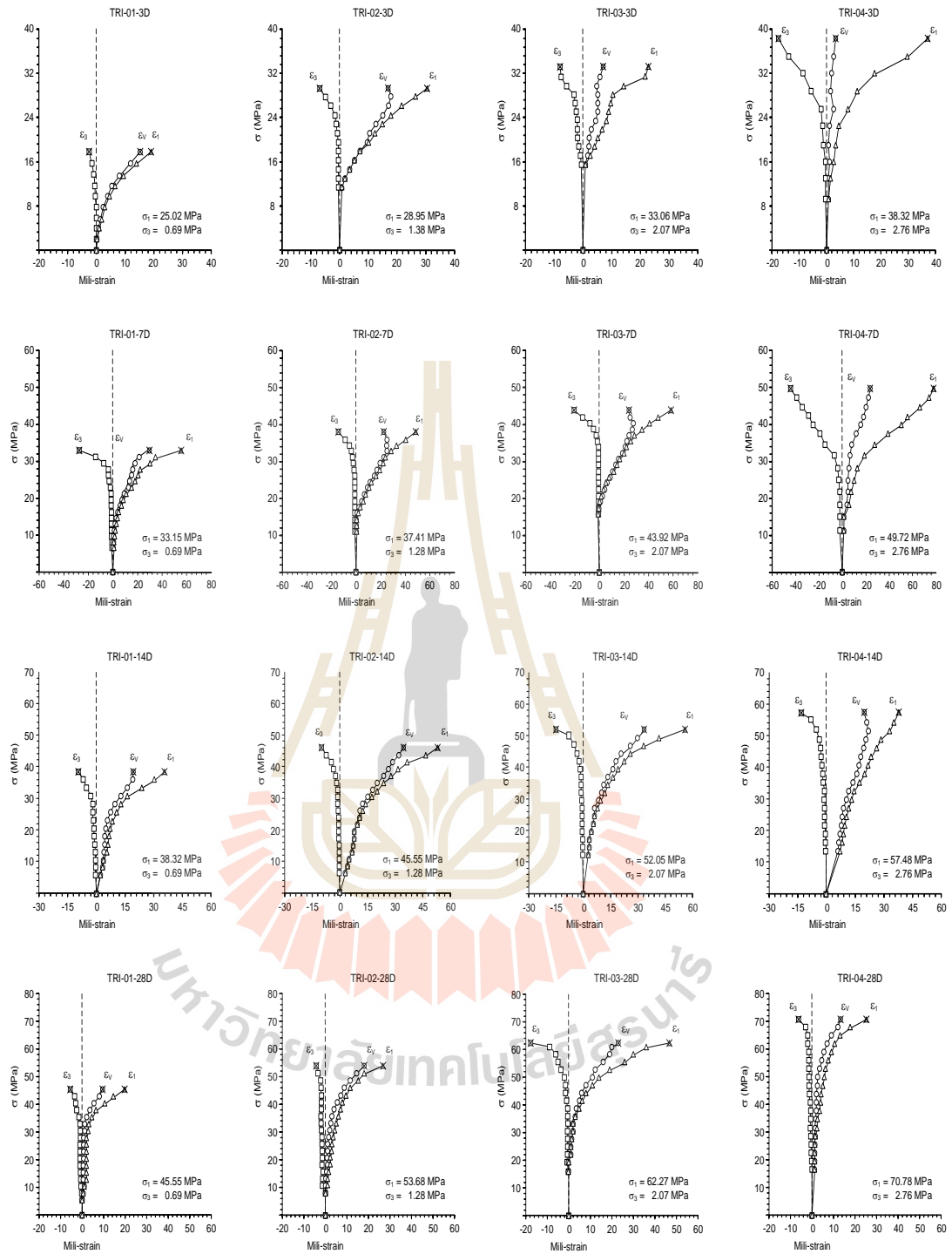


Figure 4.12 Stress-Strain curves for TRI test of CPB-1 at 3, 7, 14 and 28 days.

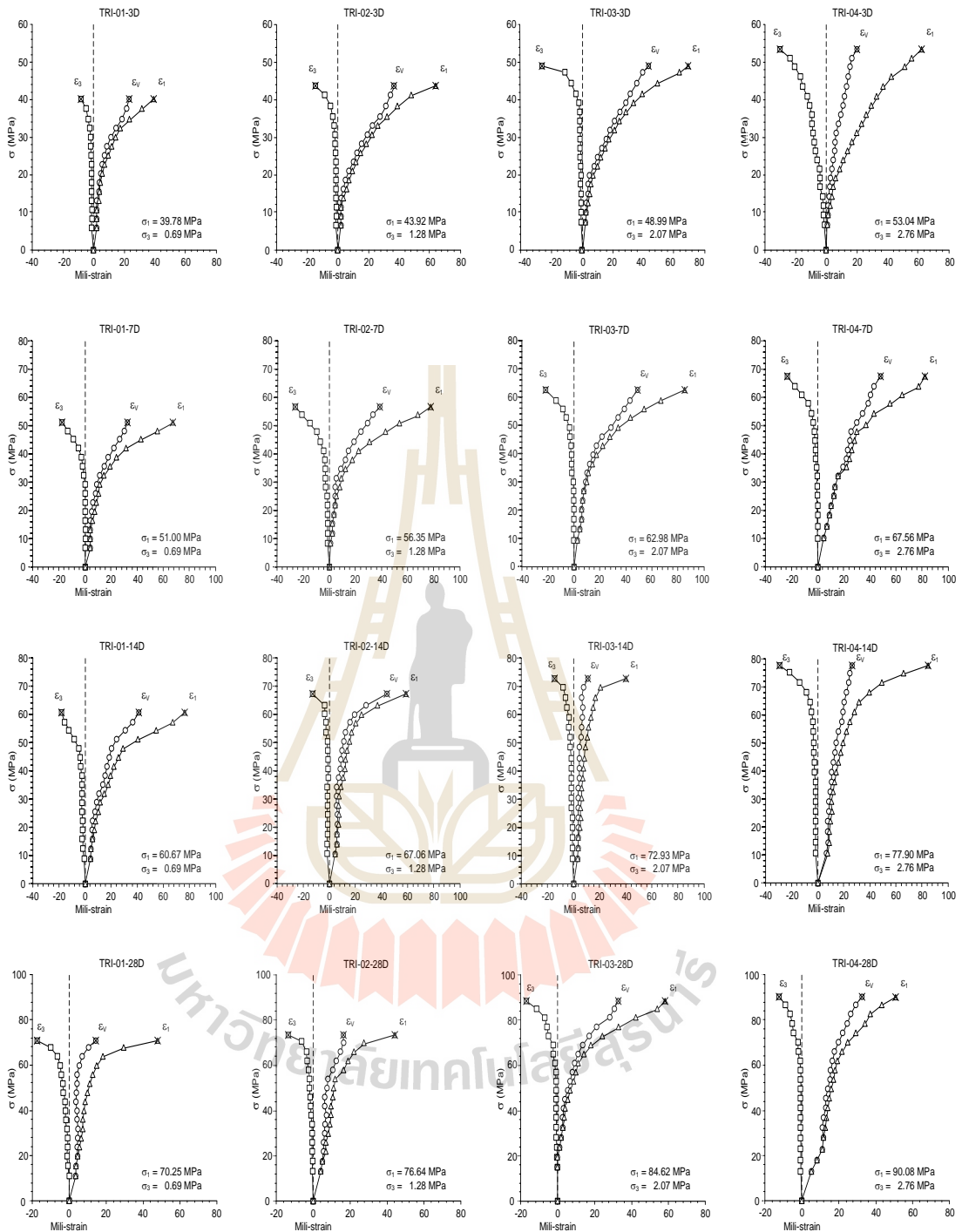


Figure 4.13 Stress-Strain curves for TRI test of CPB-1 at 3, 7, 14 and 28 days.

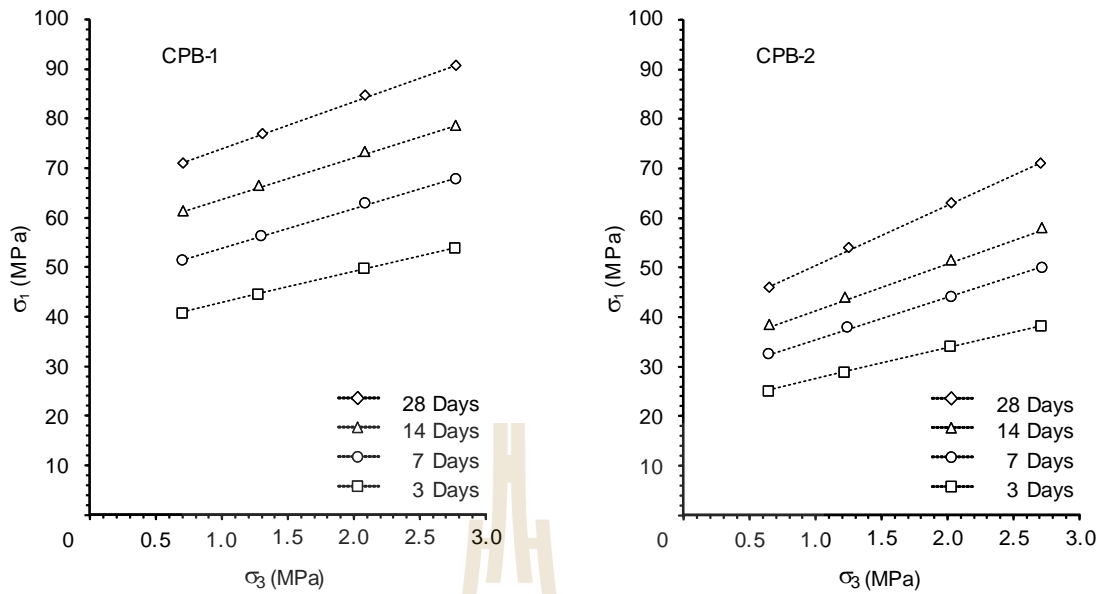


Figure 4.14 The strength development of CPB mixtures with curing period.

Table 4.7 Normal stress (σ_1) and confining pressure (σ_3) of CPB-1 mixture.

Confining pressure, σ_3 (MPa)	Normal stress, σ_1 (MPa) at curing time			
	3 days	7 days	14 days	28 days
0.69	39.78	51.00	60.67	70.25
1.28	43.92	56.35	67.06	76.64
2.07	48.99	62.98	72.93	84.62
2.18	53.04	67.56	77.90	90.08

Table 4.8 Normal stress (σ_1) and confining pressure (σ_3) of CPB-2 mixture.

Confining pressure, σ_3 (MPa)	Normal stress, σ_1 (MPa) at curing time			
	3 days	7 days	14 days	28 days
0.69	25.02	33.15	38.32	45.55
1.28	28.95	37.41	45.55	53.68
2.07	33.06	43.92	52.05	62.27
2.18	38.32	49.72	57.48	70.78

The cohesion, c and internal friction angle, ϕ are determined by the Coulomb failure criterion in terms of the principal stresses (σ_1 , σ_3) as expressed in equation (4.3) (Jaeger et al., 2007):

$$\sigma_1 = 2c \tan \beta + \sigma_3 \tan^2 \beta = 2c \tan (45 + \phi/2) + \sigma_3 \tan^2 (45 + \phi/2) \quad (4.3)$$

where σ_1 is the normal stress (MPa), σ_3 is the confining pressure (MPa), c is the cohesion (MPa) and ϕ is the internal friction angle (Degrees).

The cohesion and internal friction angle of both mixtures at each curing periods are summarized in Figure 4.15 and Table 4.9. The values are gradually increased in the first two weeks and then tend to remain constant after 28 days. In spite of not much difference in friction angle of both mixtures at each curing periods, cohesion results are obviously different. According to the Table 4.8, the CPB-1 mixtures can yield roughly twice of cohesion strength by CPB-2 mixtures.

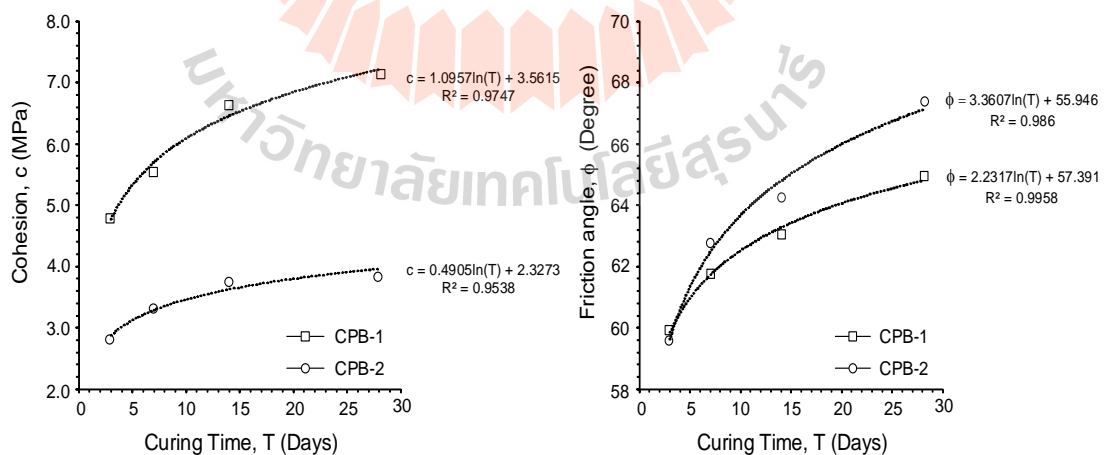
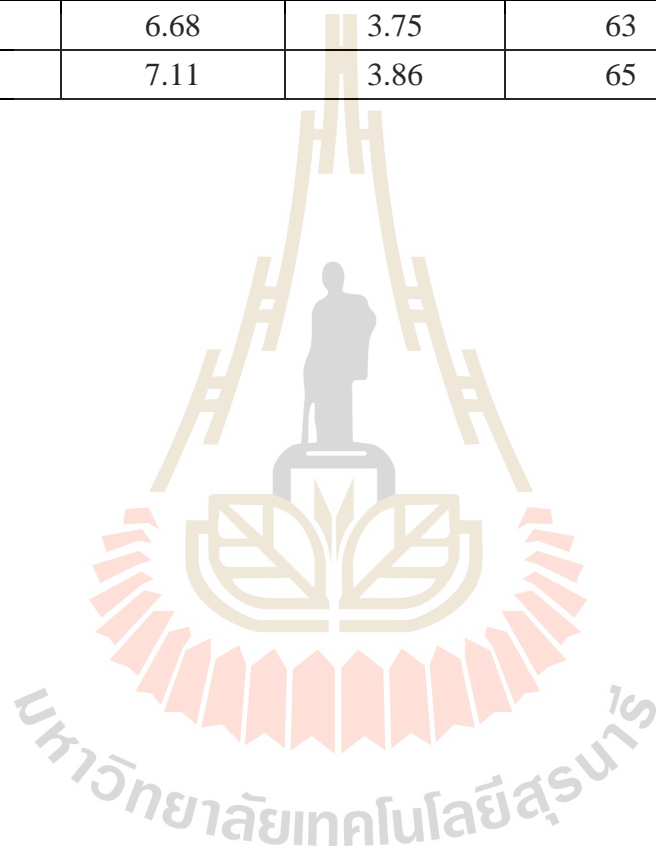


Figure 4.15 Cohesion and Internal friction angle of CPB mixtures with curing period.

Table 4.9 Cohesion and internal friction angle of CPB mixtures at each curing period.

Curing time (Days)	Cohesion, c (MPa)		Internal friction angle, ϕ (Degrees)	
	CPB-1	CPB-2	CPB-1	CPB-2
3	4.79	2.81	60	60
4	5.54	3.31	62	63
14	6.68	3.75	63	64
28	7.11	3.86	65	67



CHAPTER V

COMPUTER SIMULATION

5.1 Introduction

The computer simulation (FLAC 4.0-Itasca, 1992) is used to determine the effectiveness of sealing materials in salt and potash mines after the mine excavation are completed. The surface subsidence of salt and potash mine with sealing materials are investigated.

5.2 Related studies and input parameters

Das (1989) states that the data obtained from the laboratory tests are mostly in the form of stress-time curves from creep tests; the stress is increased quickly and then remain constant while recording the steadily increasing strain. When the applied stress is increased, the nature of cracks can change through lengthening of old cracks and initiating of new ones. Therefore, calculations of stress and deformation of visco-elastic materials are required to analyze the time-dependent problems in rocks because they will creep at relatively low different stress even without fissured and defective specimen because of the movements of dislocations and intra-crystalline gliding.

Whyatt et al. (2008) predicate that deformation of underground salt and potash mines is generally time dependent, providing for gradual adjustment of strata to mining induced stresses. If creep deformation can shift stress and potential energy to strong and brittle geologic units, the violent eventual failure will be occurred. Timely

placement of a “large volume” of backfill has certain merits for prevention of further catastrophic consequences.

Figure 5.1 expresses an example of the stratigraphic column of rock salt and clastic rock at Ban Hhao, Muang district, Udon Thani province (borehole no. K-089) (Suwanich et al., 1986).

Usually rock salt is the isometric crystals form of sodium chloride (NaCl) which is especially in cube form and usually found in massive sedimentary beds, but it can also be granular, fibrous and compact. At that time, potash is in water-soluble form that contain potassium. After the water evaporated, the potassium salts crystallized into beds of potash ore. The deposits are a naturally occurring mixture of potassium chloride (KCl) and sodium chloride (NaCl). Over time, as the surface of the earth changed, these deposits were covered by thousands of feet of earth.

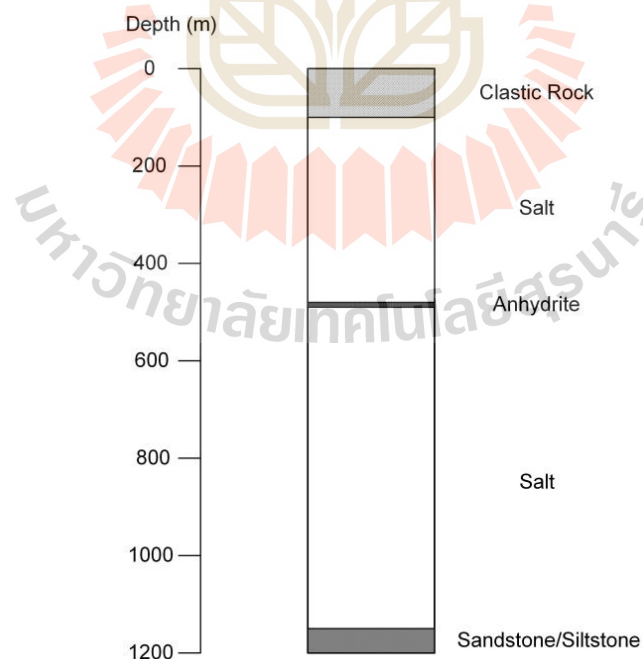


Figure 5.1 Stratigraphy of borehole no. K-089 at Ban Hhao, Muang district, Udon Thani province (Suwanich et al., 1986).

Suwanich (2007) studies the potash-evaporite deposits in the northeastern portion of Thailand; Khorat plateau. The Khorat plateau is divided into 2 basins; the north basin or Sakhon Nakhon basin and the south basin or Khorat basin. The potash minerals are deposited in the Maha Sarakham Formation which is the rock salt main deposits. The Maha Sarakham Formation is consisted of 3 layer salt beds; the Upper, Middle and Lower salt layers. These salt beds are interbedded by clastic sediments of sticky reddish brown mainly clay. The potash minerals have been found only at the top of the Lower Salt interlocking with halite or rock salt grains.

In this study, the finite difference analysis using FLAC 4.0 with Burger model is used to determine the effectiveness of sealing materials in salt and potash mines after the mine excavation was completed. This simulation can predict the elastic, visco-elastic, visco-plastic, strain-softening and dilation behavior of geological materials. Figure 5.2 shows the modular components of the Burgers model used in this computation and their output result from the time-dependent analysis.

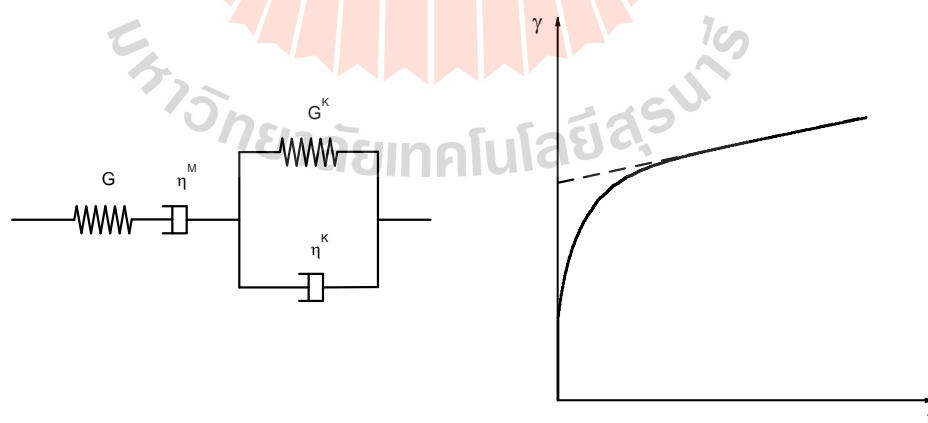


Figure 5.2 The modular components and their output result from the time-dependent analysis of the Burgers model (Goodman, 1989).

Goodman (1989) evaluated the viscoelastic constants in a Burger body through unconfined compression of cylindrical rock specimens over long-term periods. The axial deformation related with time is calculated by using the following equations:

$$\varepsilon_1(t) = \frac{2\sigma_1}{9K} + \frac{\sigma_1}{3G_2} + \frac{\sigma_1}{3G_1} - \frac{\sigma_1}{3G_1} e^{-(G_1 t / \eta_1)} + \frac{\sigma_1}{3\eta_1} t \quad (5.1)$$

$$K = E / (3(1 - 2\nu)) \quad (5.2)$$

$$G_2 = E / (2(1+\nu)) \quad (5.3)$$

where $\varepsilon_1(t)$ is the axial strain with time, σ_1 is the axial stress (MPa), K is the bulk modulus (MPa), G_2 is the elastic shear modulus (MPa), E is the elastic modulus (MPa), ν is the Poisson's ratio, and G_1 and η_1 are the constants which control and determine the amount of delayed elasticity.

The rock layer for this study excavation is considered in rock salt rather than potash because sometimes there is no overlying potash zone since the salt had flowed up as a dome until the potash zone had been dissolved completely, with no thick upper clastic covering. The Lower Salt was always located at a lower depth indicating it was a salt basin, whereas the higher elevation of the Lower Salt (mostly in the one-salt-bed holes) indicated a salt dome, usually have one salt bed (Suwanich, 2010).

Figure 5.3 also shows the different types of salt layers which were collected from a 1,200 m long profile in the shaft of the Bamnet Narong (Asian Potash Mine), Chaiyaphum Province in northeastern Thailand.

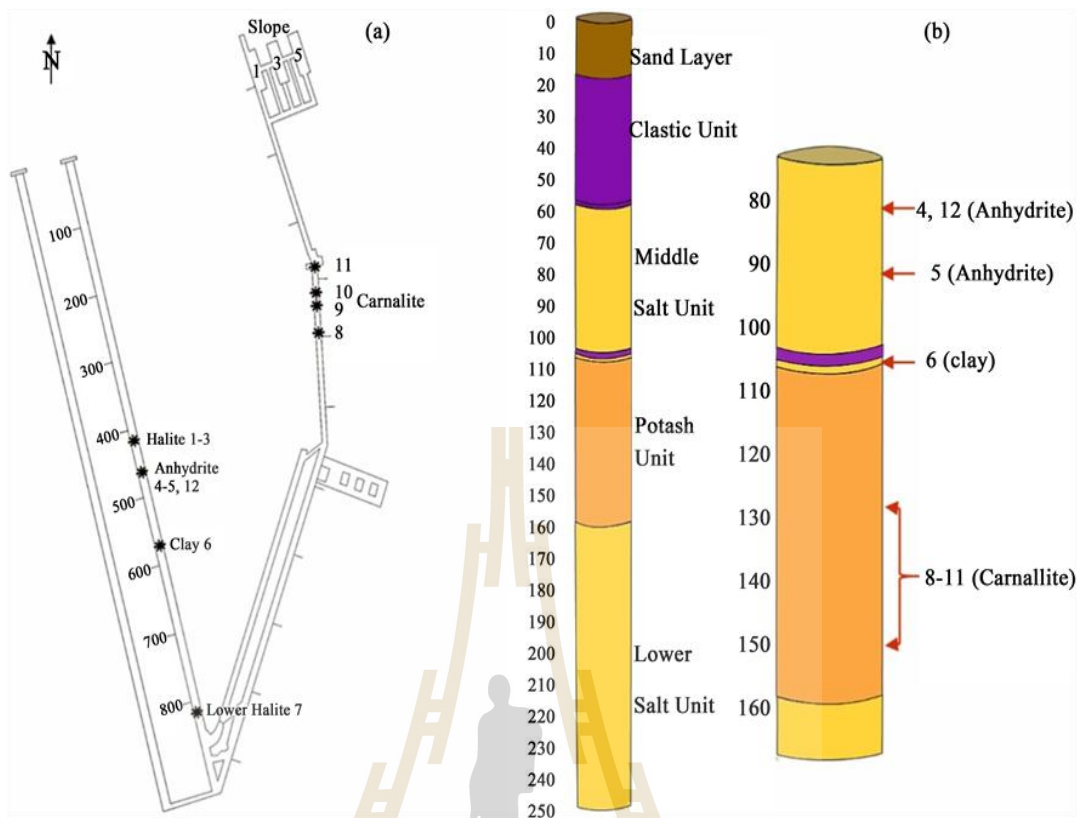


Figure 5.3 Vertical distribution of the different salt layers at Bamnet Narong, Chaiyaphum Province (Hansel et al., 2016).

The proposed finite difference mesh constructed to represent vertical model with the mine depth of 250m and opening depth and width of 10m and 8m is shown in Figure 5.4. There are 500 to 700 elements covering the cross-section of the model. In which, small elements are provided near the opening boundaries to obtain detailed behavior of the surrounding rocks and larger elements are used in the region far from the openings because stress and strain gradients are lower in these areas.

The material property parameters of rock salts used for the computer simulations are obtained from the calibration by Samsri et al. (2010) and Sriapai et al. (2012) and the clastic rock properties are taken from Crosby (2007) which are described

Table 5.1 Visco-elastic and visco-plastic properties of rock salt for FLAC 4.0 simulations (Samsri et al., 2010).

Parameters	Values
Elastic modulus, E_1 (GPa)	1.90
Spring constant in visco-elastic phase, E_2 (GPa)	5.79
Visco-plastic coefficient in steady-state phase, η^K (GPa.day)	0.34
Visco-plastic coefficient in transient phase, η^M (GPa.day)	0.71
Density, ρ (kg/m ³)	2,150

Table 5.2 Mechanical properties of clastic rock and rock salt for FLAC 4.0 simulations (Crosby, 2007, Sriapai et al, 2012).

Parameters	Rock types	
	Clastic rock	Rock salt
Density, ρ (kg/m ³)	2,490	2,150
Bulk modulus, K (GPa)	1.70	2.22
Shear modulus, G (GPa)	0.30	1.67
Cohesion, c (MPa)	3.50	0.50
Internal friction angle, ϕ (Degrees)	25	50
Tension, T (MPa)	0.83	1.00

Table 5.3 Mechanical properties of CPB mixtures for FLAC 4.0 simulations.

Parameters	Sealing materials	
	CPB-1	CPB-2
Density, ρ (kg/m ³)	1897	1881
Elastic modulus, E (MPa)	11.00	8.08
Poisson's ratio, ν	0.22	0.3
Cohesion, c (MPa)	7.11	3.86
Internal friction angle, ϕ (Degrees)	65	67
Tension, T (MPa)	1.115	0.859

By the observation of mechanical properties shown in Table 5.3 of both CPB-1 and CPB-2 mixtures, it can be definitely described that CPB-1 mixture is way better than to use as sealing material in mining. Aside from the conception of laboratory testing in which precise methods are required to show the more strength producing materials, assumption can be made in the computer simulations. Although deficient materials are used in the simulations, they can show the excepted circumstance because they can show their reliable results computed by using the input data. In consequence with this statement, the mechanical properties of CPB-2 mixture is used as an input parameters in this computer simulations.

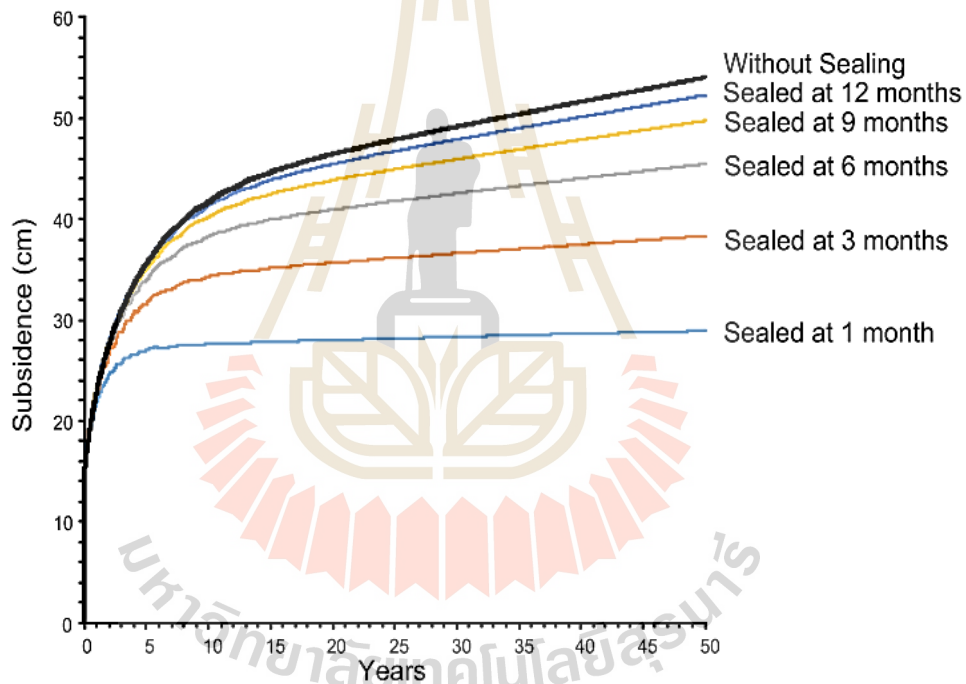
The simulation is carried out to predict the deformation behavior with and without sealing materials in mine ground under long-term interest of 50 years after mining. The time to seal in mine is also considered in this study because the suggested CPB mixtures can be prepared and placed right away when mine process are finished. The magnitudes of surface subsidence with sealing time at 1, 3, 6, 9, and 12 months are considered in this calculation.

5.3 Simulation results

The computer simulations are calculated up to 50 years after sealing in mine with the time to seal in mine of 1, 3, 6, 9 and 12 months. The effect of the CPB-2 mixture on surface subsidence reduction are considered in this section. Table 5.4 clarifies the different resulted surface subsidence at each considered sealing time. Figure 5.5 also shows the calculated surface subsidence after 50 years of prediction in selected mine with overturn thickness of 250 m and opening depth and width of 10m and 8m, and sealing time at 1, 3, 6, 9 and 12 months.

Table 5.4 Subsidence reduction with the function of sealing time.

Sealing Conditions	Subsidence (cm) at 50 Years	Reduction of Subsidence
Without sealing	54.04	-
Sealed at 1 month	28.92	46%
Sealed at 3 months	38.31	29%
Sealed at 6 months	45.46	16%
Sealed at 9 months	49.74	8%
Sealed at 12 months	52.27	3%

**Figure 5.5** Surface subsidence as a function of time with overturn thickness = 250 m and opening height = 10 m.

According to both Figure and Table, if CPB-2 mixtures are applied at 1 month after mining, the magnitude of surface subsidence is reduced as good as 46%, from about 54 cm to 29 cm, than without sealing. After all sealing at other times can reduce

the subsidence, the amount of reduction is obviously smaller when compared with 1 month result. While 29% reduction of surface subsidence is observed at 3 months (from 54 cm to 38 cm), surface subsidence can only be reduced about 9cm (16%); 54.04 cm without sealing to 45.46 cm at 6 months.

After 6 months of mine excavation, sealing has insignificant effect on the subsidence reduction. During that time the subsidence is already extend in the mine zone. There is only 8% reduction at 9 months and only 2 cm or 3% reduction is occurred when it is sealed after one year. It can obviously be described that the sealing time has the specific effect on the reduction of surface subsidence in mining.

In spite of all the results obtained from the computer simulations, the recommended CPB mixtures are applicable in reality. Without regard to the fact, the use of inferior CPB-2 mixture as a typical material in computer simulations, they give the reasonable result to use in mining design because they already have the sufficient mechanical properties to prevent the indefinite prolongation of surface subsidence by supporting room and pillar. Moreover, the mechanical properties of CPB-1 mixture should also be considered in simulations to designate the more desirable recommendation.

CHAPTER VI

DISCUSIONS, CONCLUSIONS AND RECOMMENDATIONS FOR FUTURE STUDIES

6.1 Discussions and conclusions

In this section, the results of the study of the utilization of sugarcane bagasse ash (SCBA) as cement replacement material in the mixture of SCBA, cement, bentonite and crushed salt are discussed. Moreover, it can be concluded that its strength and toughness development helping to use as cemented paste backfill (CPB) and reduce the subsidence in salt and potash mine. Many laboratory tests are performed to assess the chemical, physical and mechanical properties of CPB mixtures.

At first, the chemical compositions of the four raw materials and also CPB mixtures at 3, 7 and 30 days are determined by using X-ray fluorescence method. This method is required to analyze how much reactive silica of SCBA can help in the cement reaction with brine to produce more strength. The cement used in this study is ASTM Type V, high sulfate resistant Portland cement and SCBA is imported from Mitr Phol Phu Luang mill in Leoi Province, Thailand. Crushed salts are from the Lower members of the Maha Sarakham Formation in the Korat basin, northeastern Thailand.

In this method, nine chemical compounds are analyzed. The high silica contents in SCBA and bentonites prove that their reliability of pozzolanic reaction. Although cement, SCBA and bentonites have a small amount of sodium oxide and chloride in their chemical composition, crushed salts have a great amount which can affect in the

chemical reaction of four materials with brine because the amount of these compounds become the highest content in the CPB mixture at all curing states. Similarly for calcium oxide, which is highly comprised in cement even though other three have rare amount, become the third highest amount in CPB mixtures.

Porosity test is performed to determine the physical properties of CPB mixtures. Porosity is directly related with permeability so this test is required in the sealing design to minimize brine leakage in salt and potash mine. It also has effect on durability and strength of cemented mixtures that will be used as sealing materials. The porosity of both CPB mixtures used in this study reduce noticeably with time. The results clearly show that the voids within the mixtures are gradually taken out by the small particle sizes of SCBA, cement and bentonite that makes the mixture more effective and condense in practice.

The uniaxial compressive strength (UCS) test, triaxial compression (TRI) test and Brazilian tensile strength (BZ) test are performed to describe the mechanical properties of both CPB mixtures. From the UCS test, uniaxial compressive strength, dry density, Elastic modulus and Poisson's ratio of both mixtures are determined. Different from the other factors, the dry densities of both mixtures at each curing period are not much changed; all the values are about 1.8 ton/m^3 . However, elastic moduli, Poisson's ratio and UCSs of both mixtures are gradually increased with the curing periods. Even though elastic moduli of CPB-1 mixture are greater than CPB-2 mixture, the values of Poisson's ratio are lesser. When the 28-day UCS of CPB-2 is 5.12 MPa, CPB-1 can provide 5.19 MPa at only 14 days. At 28 days, it can support nearly 7 MPa. These results clearly show that the use of CPB-1 mixture is more effective than CPB-2 mixture.

The tensile strength of CPB mixtures are determined by using Brazilian tensile strength (BZ) test. The increasing tensile strength of both mixtures show their strength gain with time. According to this test, CPB-1 mixture can provide 1.5% strength more than CPB-2 mixture. It seems CPB-1 mixture is more useful than CPB-2 mixture from the tensile strength point of view.

Triaxial compression (TRI) test is used to determine the relationship between normal stress and confining pressures, cohesion, and internal friction angle of both CPB mixtures. Although the strength results of both mixtures are steadily increased with curing time, the 28-day strength of CPB-2 mixture with confining pressures of 2.76 MPa is 70.78 MPa which is nearly equal to the CPB-1 mixture with only confining pressures of 0.69 MPa at the same 28 days.

The cohesion and internal friction angle of the mixtures are gradually increased in the first two weeks and then tend to remain constant after 28 days. In spite of not much difference in friction angle, cohesion results are obviously different since the CPB-1 mixture can yield roughly twice of cohesion strength by CPB-2 mixture. The results from TRI test also prove that CPB-1 mixture is more beneficial than CPB-2 mixture. The data used in this study are recorded manually so relevant standard deviation factors should be used for all tests to obtain the precise results.

Even so, the sealing materials cannot immediately provide strength after they are placed into the opening. They can only be functional when the roof deflected as a result of inducing the vertical stresses on sealing materials. Then they are expanded around in the horizontal direction to strengthen the pillar and reduce the subsidence, pillar deformation and deformations of roof deflection. Therefore, the sealing time has the specific effect on the reduction of surface subsidence in mining because the opening

will be falling under hydrostatic stresses conditions for long-term periods. This evidence can be confirmed by the numerical simulation results.

Computer simulation is carried out to predict the deformation behavior with and without sealing materials in mine opening under long-term interest of 50 years after mining. For modelling, finite difference mesh with overburden thickness of 250 m, opening depth and width of 10 m and 8m is considered with sealing time at 1, 3, 6, 9 and 12 months. For calculation, the required input parameters of rock in model are resulted values of the rock salt which has usually higher strength and elastic values than potash formation and the sealing materials are CPB-2 mixtures.

According to the engineering point of view, if the lower strength materials can resist the stress, the accurate materials with more strength can surely withstand more stresses. Therefore, CPB-2 mixture is selected as a representative sealing material for the computer simulation in this study because its strength is lower than that of CPB-1 mixture.

When CPB-2 mixtures are applied at 1 month after mining, the magnitude of surface subsidence is reduced virtually 46%, from about 54 cm to 29 cm, than without sealing. Sealing at other times can also reduce the subsidence, but the amount of reduction is smaller when compared with 1 month result. On the other hand, if CPB-1 mixture is used instead of CPB-2 mixture for sealing, the surface subsidence of CPB-1 mixture will be reduced more than that of CPB-2 mixture. The reason is that the strength and toughness values of CPB-1 mixture are already higher than those of CPB-2 mixture.

6.2 Recommendations for futures studies

This study may have limitations to enhance as a result the following future studies are suggested:

1. The various composition of four materials; SCBA, cement, bentonites and crushed salt should be performed.
2. The different types of pozzolanic materials such as fly ash, rice husk ash, wheat straw ash, hazel nutshell, natural pozzolans, slags, and silica fume should be composed in the mixture.
3. Curing time should be longer (months or years) for long-term effect on strength and toughness development to make sure the chemical reaction reach their optimum state.
4. Shear strengths of the mixtures should be determined.
5. Scanning electron microscopy (SEM) should be performed to understand more about the chemical reaction in the mixture.
6. More specifications such as overburden thickness, mine opening depth, room height and width, and also potash layer should be considered in the computer simulations.

REFERENCES

- Amin, N. (2011). Use of bagasse ash in concrete and its impact on the strength and chloride resistivity. **Journal of Materials in Civil Engineering**. 23(5).
- Arioglu, E. (1995). Strain of Concrete at Peak Compressive Stress for a Wide Range of Compressive Strengths, Discussion on paper by B. de Nicolo, L. Panni, E. Pozzo. **Materials and Structures**. 28(184): 611 – 614.
- ASTM C150/C150M (2016e1). Standard Specification for Portland cement. **Annual Book of ASTM Standard**, Vol.04.01. Philadelphia: American Society for Testing and Materials.
- ASTM D3967 (2008). Standard Test Method for Splitting Tensile Strength of Intact Rock Core Specimens. **Annual Book of ASTM Standards**, Vol.04.08. Philadelphia: American Society for Testing and Materials.
- ASTM D7012 (2014). Standard Test Methods for Compressive Strength and Elastic Moduli of Intact Rock Core Specimens under Varying States of Stress and Temperatures. **Annual Book of ASTM Standards**, Vol.04.09. Philadelphia: American Society for Testing and Materials.
- Balaji, K. (2015). Partial replacement of cement in concrete with sugarcane Bagasse Ash.
- Belem, T., Harvey, A., Simon, R., and Aubertin, M. (2004). Measurement and prediction of internal stresses in an underground opening during its filling with cemented fill. In **Proceedings of the 5th International Symp. on Ground support in Mining and Underground Construction**. Villaescusa & Potvin

- (eds.); 2004 Sep 28-30; Perth, Western Australia, Australia, Taylor & Francis Group, London. p. 619 – 630.
- Butcher, B.M., Novak C. F. and Jercinovic M. (1991). The advantages of a salt/bentonite backfill for Waste Isolation Pilot Plant disposal rooms. **SAND90-3074**, Sandia National Laboratories, Albuquerque, New Mexico.
- Case, J.B. and Kelsall, P. (1987). Laboratory investigation of crushed salt consolidation. **International Journal of Rock Mechanics and Mining Science and Geomechanics Abstracts** 25. (5): 216 – 223.
- Cordeiro, G.C., Toledo Filho, R.D., Tavares, L.M., Fairbairn, E.M.R. (2008). Pozzolanic activity and filler effect of sugar cane bagasse ash in Portland cement and lime mortars. **Cement and Concrete Composites**. 30: 410 – 418.
- Crosby, K. (2007). Integration of rock mechanics and geology when designing the Udon South sylvinitic mine. In **Proceedings of the First Thailand Symposium on Rock Mechanics** (pp. 3 – 22). Nakhon Ratchasima.
- Das, B.M. (2010). **Principles of Geotechnical Engineering** (Seventh edition). United States of America. pp 49 – 72.
- Domitrovic, D. and Kovacevic, Z.B. (2013). The relationship between swelling and shear strength properties of bentonites. In **Proceedings of the 18th International Conference on Soil Mechanics and Geotechnical Engineering**, Technical Committee 101 - Session I (pp. 219 – 222).
- Duncan, E.J. Scott and Emery Z. Lajtai. (1993). The creep of Potash Salt Rocks from Saskatchewan. **Geotechnical and Geological Engineering**. 11: 159 – 184.
- Fuenkajorn, K., and Daemen, J.J.K. (1987). Mechanical interaction between rock and multi-component shaft or borehole plugs: Rock mechanics. In I. W. Farmer, J.J.

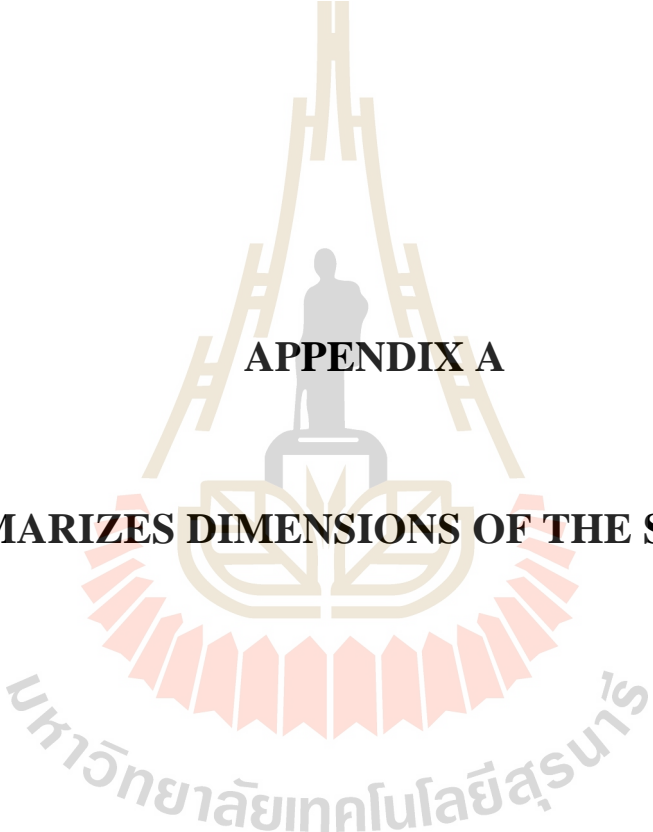
- K. Daemen, C. S. Desai, C. E. Glass, and S. P. Neuman (eds.). **Rock Mechanics Proceedings of the 28th U.S. Symposium** (pp. 165 – 172). Rotterdam: A.A. Balkema.
- Ganesan, K., Rajagopa, K. and Thangavel, K. (2007). Evaluation of bagasse ash as supplementary cementitious material. **Cement and Concrete Composites**. 29; 515 – 524.
- Goodman, R.E. (1989). **Introduction to Rock Mechanic**. (Second edition). University of California at Berkeley. pp 179 – 220.
- Hansen, B., Wemmer, K., Eckhardt, M., Putthapiban, P. and Assavapatchara, S. (2016). Isotope Dating of the Potash and Rock Salt Deposit at Bamnet Narong, NE-Thailand. **Open Journal of Geology**. 6: 875-894.
- Hansen, F.D. (1997). Reconsolidating salt: compaction constitutive modeling, and physical processes. **International Journal of Rock Mechanics and Mining Sciences**. 34 (3-4), paper No. 119.
- Idris, M.K., Yassin, K.E. (2015). Determination of the effects of Bagasse Ash on the properties of Portland cement. **Journal of Applied and Industrial Sciences**. 3(1): 6 – 11.
- Itasca (2002). **FLAC-Fast Lagrangian Analysis of Continua, Version 4.0**, User'. Itasca Consulting Group Inc., Minneapolis, MN, USA.
- Jaeger, J.C., Cook, N.G., and Zimmerman, R.W. (2007). **Fundamentals of rock mechanics**. Blackwell Publishing, fourth edition, pp 80 – 105.
- Ju, J. and Xu, J. (2015). Surface stepped subsidence related to top-coal caving longwall mining of extremely thick coal seam under shallow cover. **International Journal of Rock Mechanics & Mining Sciences**. 78: 27 – 35.

- Kelsall, P.C., Case, J.B., Coons, W.E., Franzone, J.G. and Meyer, D. (1984). Schematic designs for penetration seals for a repository in the Permian basin. WMI/ONWI-564, prepared by IT Corporation for office of Nuclear Waste Isolation. **Battelle Memorial Institute**. Columbus, Ohio.
- Kuhlman, K.L. and Malama, B. (2013). Brine Flow in Heated Geologic Salt. **SANDIA REPORT**, SAND2013-1944. U.S. Department of Commerce, National Technical Information Service, Springfield, VA.
- Landriault, D.A., Verburg, R., Cincilla, W., and Welch, D. (1997). Paste Technology for underground backfill and surface tailings disposal applications, Short Course Notes. In: **CIM Technical Workshop** – April 27, Vancouver, British Columbia, Canada, 1997.
- Li, M., Zhang, H., Xing, W. (2015). Study of the relationship between surface subsidence and internal pressure in salt caverns. **Environmental Earth Science**. 73 (11): 6899 – 6910.
- Malan, D.F. (1999). Time-dependent behavior of deep level tabulator excavations in hard rock. **Rock Mechanics and Rock Engineering**. 32(2): 123 – 155.
- Malovichko, A.A., Sabirov, R.H. and Akhmetov, B.S. (2005). Ten Years of Seismic Monitoring in Mines of the Verkhnekamskoye Potash Deposit. In **Controlling Seismic Risk: Proceedings of the Sixth International Symposium on Rockbursts and Seismicity in Mines (RaSim 6)**, 9-11 March 2005, Australia, pp. 367 – 372.
- Mier, J.G.M., Shah, S. P., Arnaud, M., Balayssac, J.P., Bascoul, A., Choi, S., Dasenbroc, D., Ferrara, G., French, C., Gobbi, M.E, Karihaloo, B.L., König, G.,

- Kotsovos, M.D., Labuz, J., Lange-Kornba, D., Markeset, G., Pavlovic, M.N., Simsch, G., Thienel, K-C., Turatsinze, A., Ulmer, M., van Geel, H.J.G.M., van Vliet, M.R.A. and Zissopoulos, D. (1997). Strain-softening of concrete in uniaxial compression. **Materials and Structures**. 30: 195 – 209.
- Mikkelsen, P.E. (2002). Cement-Bentonite Grout Backfill for Borehole Instruments. **Geotechnical Instrumentation News**, Geotechnical News, December 2002, pp. 38 – 42.
- Minkley, W. and Menzel, W. (1996). Dynamic System Stability of Mining Structures in Salt Mining. Rock Mechanics: Tools and Techniques; **Proceedings of the 2nd North American Rock Mechanics Symposium: NARMS '96**, Montreal, Canada, 19-21 June 1996. Aubertin, Hassani and Mitri (eds.). Balkema, pp. 93 – 100.
- Naik, T.R. (1997). Concrete durability as influenced by density and/or porosity. **The Cement and Concrete Institute of Mexico Symposium "World of Concrete - Mexico"**, Guadalajara, Mexico, June 4 – 7, 1997.
- Naylor, J., Famermery, R.A., and Tenbergen, R.A. (1997). Paste backfill at the macassa mine with flash paste production and storage mechanism. In **Proceedings of the 29th annual meeting of the Canadian Mineral Processors (Division of the CIM)**; 1997 Jan 21 – 23; Ottawa, Ontario.
- Sahua, P. and Lokhandeb, R.D. (2015). An investigation of sinkhole subsidence and its preventive measures in underground coal mining. **Procedia Earth and Planetary Science**. 11: 63 – 75.

- Samsri, P., Sriapai, T., Walsri, C. and Fuenkajorn, K. (2010). Polyaxial creep testing of rock salt. In **Proceedings of the Third Thailand Symposium on Rock Mechanicson** (pp. 125 – 132). Thailand.
- Schulze, J. (1999). Influence of water-cement ratio and cement content on the properties of polymer-modified mortars. **Cement and Concrete Research**. 29: 909 – 915.
- Singh, S.B., Munjal, P., and Thammishetti, N. (2015). Role of water/cement ratio on strength development of cement mortar. **Journal of Building Engineering**. 4: 94 – 100.
- Sivakugan, N., Veenstra, R., and Naguleswaran, N. (2015). Underground mine backfilling in Australia using paste fills and hydraulic fills. **International Journal of Geosynthetics and Ground Engineering**. 1: 18.
- Sriapai. T., Chaowarin, W. and Fuenkajorn, K. (2012). Effects of temperature on compressive and tensile strengths of salt. **Science Asia**. 38: 166 – 174.
- Suwanich, P. (2007). Potash-evaporite deposits in Thailand. In **Proceedings of the International Conference on Geology of Thailand** (pp. 252-262). 21-22 November 2007, Department of Mineral Resources, Thailand.
- Suwanich, P. (2010). Geology and Geological Structure of Potash and Rock Salt Deposits in Chalerm Phrakiat District, Nakhon Ratchasima Province in Northeastern Thailand. **Kasetsart Journal (Natural Science)**. 44: 1058 – 1068.
- Suwanich, P. and Ratanajaruraks, P. (1986). Sequences of rock salt and potash in Thailand (Nonmetallic Minerals Bulletin No. 1). Bangkok: Economic Geology, Division. **Department of Mineral Resources**. Bangkok.

- Tariq, A. and Yanful, E.K. (2013). A review of binders used in cemented paste tailings for underground and surface disposal practices. **Journal of Environmental Management**. 131: 138 – 149.
- Vu, X.H., Malecot, Y., and Daudeville, L. (2009). Strain measurements on porous concrete samples for triaxial compression and extension tests under very high confinement. **Journal of Strain Analysis for Engineering Design**. 44: 633 – 657.
- Vu, X.H., Malecot, Y., Daudeville, L., and Buzaud, E. (2009b). Effect of the water/cement ratio on concrete behavior under extreme loading. **International Journal for Numerical and Analytical Methods in Geomechanics**. 33: 1867 – 1888.
- Whyatt, J. and Varley, F. (2008). Catastrophic failures of underground evaporite mines. In **Proceedings Twenty-seventh International Conference on Ground Control in Mining**, 113–122, Morgantown, ICGCM.
- Yun-Yong, K., Kwang-Myung, L., Jin-Wook, B., and Seung-Jun, K. (2014). Effect of W/C ratio on durability and porosity in cement mortar with constant cement amount. **Advances in Materials Science and Engineering**. 1 – 11.
- Yurtdas, I., Burlion, N. and Skoczylas, F. (2004). Experimental characterization of the drying effect on uniaxial mechanical behavior of mortar. **Materials and Structures**. 37(267): 170 – 176.



APPENDIX A

SUMMARIZES DIMENSIONS OF THE SPECIMEN

Table A.1 Specimen dimensions of CPB-1 mixture for Porosity test.

Specimen No.	Diameter (mm)	Length (mm)	Wight (mm)	Density (g/cc)
P-3D-01	4.1	4.2	91.18	1.644
P-3D-02	4.1	4.3	92.23	1.625
P-3D-03	4.1	4.2	91.25	1.646
P-7D-01	4.1	4.5	99.87	1.681
P-7D-02	4.1	4.8	107.27	1.693
P-7D-03	4.1	4.6	100.58	1.656
P-14D-01	4.1	5.0	110.35	1.672
P-14D-02	4.1	5.1	118.12	1.754
P-14D-03	4.1	5.0	112.50	1.704
P-28D-01	4.1	5.8	135.5	1.770
P-28D-02	4.1	5.8	138.9	1.814
P-28D-03	4.1	5.9	141.0	1.841

Table A.2 Specimen dimensions of CPB-2 mixture for Porosity test.

Specimen No.	Diameter (mm)	Length (mm)	Wight (mm)	Density (g/cc)
P-3D-01	4.1	4.2	85.18	1.536
P-3D-02	4.1	4.3	86.34	1.521
P-3D-03	4.1	4.2	85.30	1.538
P-7D-01	4.1	4.5	93.87	1.580
P-7D-02	4.1	4.8	102.27	1.614
P-7D-03	4.1	4.6	94.58	1.557
P-14D-01	4.1	5.0	103.89	1.574
P-14D-02	4.1	5.1	109.49	1.626
P-14D-03	4.1	5.0	107.12	1.623
P-28D-01	4.1	5.8	130.15	1.700
P-28D-02	4.1	5.8	131.75	1.721
P-28D-03	4.1	5.9	135.17	1.735

Table A.3 Specimen dimensions of CPB-1 mixture for UCS test.

Specimen No.	Diameter (mm)	Length (mm)	Wight (mm)	Density (g/cc)
UCS-3D-01	55.5	137.0	604.5	1.825
UCS-3D-02	56	136.5	604.0	1.797
UCS-3D-03	56	137.0	607.5	1.801
UCS-7D-01	54.0	135.0	549.5	1.778
UCS-7D-02	55.5	136.0	606.0	1.843
UCS-7D-03	56.0	136.0	607.0	1.813
UCS-14D-01	54.0	135.0	555.5	1.798
UCS-14D-02	56.0	135.0	601.5	1.810
UCS-14D-03	55.0	136.0	606.0	1.876
UCS-28D-01	55.0	135.5	606.5	1.885
UCS-28D-02	56.0	136.0	611.0	1.825
UCS-28D-03	55.0	136.0	610.5	1.890

Table A.4 Specimen dimensions of CPB-2 mixture for UCS test.

Specimen No.	Diameter (mm)	Length (mm)	Wight (mm)	Density (g/cc)
UCS-3D-01	55.0	135.1	584.5	1.822
UCS-3D-02	53.5	134.9	590.5	1.948
UCS-3D-03	54.2	135.0	582.5	1.871
UCS-7D-01	53.5	135.0	591.5	1.950
UCS-7D-02	56.0	135.2	592.5	1.780
UCS-7D-03	54.2	135.0	547.0	1.757
UCS-14D-01	53.5	134.6	546.0	1.805
UCS-14D-02	54.0	136.0	596.5	1.916
UCS-14D-03	54.0	135.0	592.0	1.916
UCS-28D-01	53.5	135.8	577.5	1.893
UCS-28D-02	53.0	135.0	561.5	1.886
UCS-28D-03	54.0	136.0	580.0	1.863

Table A.5 Specimen dimensions of CPB-1 mixture for BZ test.

Specimen No.	Diameter (mm)	Length (mm)	Wight (mm)	Density (g/cc)
BZ-3D-01	54.0	26.8	113.0	1.842
BZ-3D-02	55.5	27.0	121.5	1.861
BZ-3D-03	56.0	27.0	123.0	1.851
BZ-3D-04	54.0	27.0	113.5	1.836
BZ-3D-05	55.0	27.5	120.0	1.838
BZ-3D-06	55.0	27.0	123.5	1.926
BZ-3D-07	56.0	26.8	124.5	1.887
BZ-3D-08	53.5	26.8	113.0	1.877
BZ-3D-09	55.5	28.0	124.0	1.832
BZ-3D-10	54.0	27.5	114.0	1.811
BZ-7D-01	56.0	27.0	120.0	1.805
BZ-7D-02	55.5	28.0	124.5	1.839
BZ-7D-03	56.0	28.0	125.0	1.813
BZ-7D-04	55.5	27.0	119.0	1.823
BZ-7D-05	55.5	27.0	119.5	1.830
BZ-7D-06	56.0	27.5	123.0	1.817
BZ-7D-07	53.5	27.5	111.0	1.796
BZ-7D-08	56.0	28.0	126.0	1.828
BZ-7D-09	54.0	27.0	112.0	1.812
BZ-7D-10	53.5	28.0	115.5	1.836
BZ-14D-01	56.0	27.5	123.0	1.817
BZ-14D-02	56.0	27.0	121.0	1.820
BZ-14D-03	54.0	26.5	110.5	1.822
BZ-14D-04	55.0	27.0	110.5	1.723
BZ-14D-05	55.5	27.0	120.5	1.846
BZ-14D-06	56.0	27.0	122.0	1.835
BZ-14D-07	54.0	26.5	107.0	1.764
BZ-14D-08	56.0	27.0	123.5	1.858
BZ-14D-09	56.0	27.0	120.0	1.805
BZ-14D-10	56.0	27.5	120.5	1.780
BZ-28D-01	56.0	26.5	117.5	1.801
BZ-28D-02	53.5	26.8	116.5	1.935

Table A.5 Specimen dimensions of CPB-1 mixture for BZ test (Cont.).

Specimen No.	Diameter (mm)	Length (mm)	Wight (mm)	Density (g/cc)
BZ-28D-03	56.0	27.0	122.5	1.843
BZ-28D-04	56.0	27.0	122.0	1.835
BZ-28D-05	54.0	27.0	113.5	1.836
BZ-28D-06	53.0	27.0	112.0	1.881
BZ-28D-07	53.0	26.5	111.5	1.908
BZ-28D-08	54.0	27.0	116.5	1.885
BZ-28D-09	56.0	27.0	119.5	1.798
BZ-28D-10	53.5	27.0	114.0	1.879

Table A.6 Specimen dimensions of CPB-2 mixture for BZ test.

Specimen No.	Diameter (mm)	Length (mm)	Wight (mm)	Density (g/cc)
BZ-3D-01	53.5	26.8	105.0	1.744
BZ-3D-02	54.0	27.0	108.0	1.747
BZ-3D-03	54.0	27.0	117.0	1.893
BZ-3D-04	54.0	27.0	112.0	1.812
BZ-3D-05	56.0	27.4	118.0	1.749
BZ-3D-06	54.2	27.2	116.0	1.849
BZ-3D-07	56.0	26.8	119.0	1.804
BZ-3D-08	54.2	26.8	117.0	1.893
BZ-3D-09	53.5	27.0	99.0	1.632
BZ-3D-10	54.0	27.0	114.0	1.845
BZ-7D-01	53.5	27.0	108.5	1.788
BZ-7D-02	53.5	27.0	108.5	1.788
BZ-7D-03	54.0	27.0	109.0	1.764
BZ-7D-04	54.0	27.0	109.5	1.772
BZ-7D-05	53.5	27.0	108.5	1.788
BZ-7D-06	54.0	27.0	109.5	1.772
BZ-7D-07	55.0	27.0	112.0	1.747
BZ-7D-08	55.0	27.0	110.5	1.723
BZ-7D-09	56.0	27.0	112.5	1.693

Table A.6 Specimen dimensions of CPB-1 mixture for BZ test (Cont.).

Specimen No.	Diameter (mm)	Length (mm)	Wight (mm)	Density (g/cc)
BZ-7D-10	56.0	27.0	112.0	1.685
BZ-14D-01	53.5	26.8	108.0	1.794
BZ-14D-02	54.0	27.0	109.5	1.772
BZ-14D-03	54.2	27.1	112.0	1.792
BZ-14D-04	53.5	26.0	108.5	1.857
BZ-14D-05	55.0	26.9	113.0	1.769
BZ-14D-06	54.0	27.0	109.5	1.772
BZ-14D-07	54.2	27.0	112.0	1.799
BZ-14D-08	55.0	27.0	120.0	1.872
BZ-14D-09	56.0	27.1	120.0	1.799
BZ-28D-10	56.0	27.2	122.0	1.822
BZ-28D-01	55.5	27.0	113.5	1.739
BZ-28D-02	53.5	26.8	104.5	1.735
BZ-28D-03	53.5	26.8	101.5	1.686
BZ-28D-04	53.5	27.0	110.5	1.821
BZ-28D-05	54.0	27.0	107.0	1.731
BZ-28D-06	53.5	27.0	101.0	1.665
BZ-28D-07	54.0	27.0	103.0	1.667
BZ-28D-08	56.0	26.9	111.0	1.676
BZ-28D-09	56.0	27.1	117.0	1.754
BZ-28D-10	54.0	27.0	105.5	1.707

Table A.7 Specimen dimensions of CPB-1 mixture for TRI test.

Specimen No.	Diameter (mm)	Length (mm)	Wight (mm)	Density (g/cc)
TRI-3D-01	53.0	106.5	427.0	1.818
TRI-3D-02	53.5	106.0	424.0	1.780
TRI-3D-03	52.5	107.0	411.5	1.777
TRI-3D-04	53.0	107.0	416.5	1.765
TRI-7D-01	53.2	107.0	425.5	1.790
TRI-7D-02	53.0	106.0	430.5	1.842

Table A.7 Specimen dimensions of CPB-1 mixture for TRI test (Cont.).

Specimen No.	Diameter (mm)	Length (mm)	Wight (mm)	Density (g/cc)
TRI-7D-03	53.0	107.0	422.5	1.791
TRI-7D-04	53.8	107.0	423.0	1.740
TRI-14D-01	54.0	106.0	422.0	1.739
TRI-14D-02	54.0	108.0	421.5	1.705
TRI-14D-03	53.0	108.5	430.0	1.797
TRI-14D-04	53.0	107.0	419.5	1.778
TRI-28D-01	54.0	106.8	432.5	1.782
TRI-28D-02	54.0	106.0	434.0	1.756
TRI-28D-03	54.0	106.0	421.0	1.760
TRI-28D-04	53.8	105.0	435.0	1.844

Table A.8 Specimen dimensions of CPB-2 mixture for TRI test.

Specimen No.	Diameter (mm)	Length (mm)	Wight (mm)	Density (g/cc)
TRI-3D-01	53.5	108.0	433.0	1.784
TRI-3D-02	53.8	108.2	449.0	1.826
TRI-3D-03	54.0	108.0	473.5	1.915
TRI-3D-04	54.0	106.5	429.0	1.760
TRI-7D-01	53.0	106.0	420.5	1.799
TRI-7D-02	53.5	107.0	470.0	1.955
TRI-7D-03	53.5	108.0	473.0	1.949
TRI-7D-04	53.0	107.0	412.0	1.746
TRI-14D-01	54.0	108.0	435.0	1.760
TRI-14D-02	53.5	107.9	439.0	1.811
TRI-14D-03	53.5	108.0	440.0	1.813
TRI-14D-04	54.0	107.0	429.0	1.752
TRI-28D-01	53.5	108.0	432.5	1.782
TRI-28D-02	53.5	108.0	424.0	1.747
TRI-28D-03	54.0	108.0	458.5	1.855
TRI-28D-04	53.8	107.0	435.0	1.789

BIOGRAPHY

Ms. Ei Ei San was born on November 4, 1993 in Insein Township, Yangon Region, Myanmar. She studied the civil engineering at the undergraduate course at Technological University (Hmawbi) and received her Bachelor of Technology (Civil) in 2014. In 2015, she was awarded the scholarship from Thailand International Cooperation Agency (TICA) to apply for the Master of Geotechnical Engineering at the Suranaree University of Technology under the 3-year HRD program of the Technical Cooperation Framework between Myanmar and Thailand (2013 – 2015).

